Chemical and spectroscopic characterization of (Artemisinin/Quercetin/Zn) mixed ligand complex with assessment of its potent high antiviral activity against "SARS-CoV-2" and antioxidant capacity against toxicity induced by acrylamide in male rats

Samy M. El-Megharbel[1]†, Safa H. Qahl[2], Bander Albogami[3], Reham Z. Hamza[3]*†

[1]Department of Chemistry, College of Sciences, Taif University, P.O. Box 11099, Taif 21944, Saudi Arabia
[2]Department of Biology, College of Science, University of Jeddah, P.O. Box 80327, Jeddah 21589, Saudi Arabia
[3]Department of Biology, College of Sciences, Taif University, P.O. Box 11099, Taif 21944, Saudi Arabia

*Corresponding author: Prof. Dr. Reham Zakaria Hamza
E-mail: dr_reham_z@yahoo.com, Reham.z@tu.edu.sa
†These authors contributed equally to this work.

Abstract: A novel Zn/Artemisinin/Quercetin (Art/Q/Zn) mixed ligand complex has been synthesized, tested for its viral inhibition against (SARS-CoV-2) and investigated for its effect against toxicity and oxidative stress induced by acrylamide (Acy), which is formed when starchy foods are cooked at high temperatures. The synthesized complex was chemically characterized by (elemental analysis, conductance measurements, FT-IR, UV, magnetic measurements and XRD). Surface morphology of the Art/Q/Zn complex was investigated by scanning and transmission electron microscopy (SEM, TEM), as well as energy dispersive X-ray analysis. The Art/Q/Zn complex has been tested *in vitro* to estimate its antiviral activity against SARS-CoV-2 and *in vivo* against toxicity induced by Acy on both hepatic and pulmonary tissues. An experimental model was used to evaluate the ameliorative effect of the Art/Q/Zn complex on both lung and liver toxicity of Acy. Forty male rats were divided randomly into four groups: control; Acy (500 mg/Kg); Art/Q/Zn (30 mg/kg) and a combination of Acy and Art/Q/Zn, The complex was administered orally for a successive period of 30 days. Hepatic functions, inflammation marker (CRP), tumour necrosis factor, interleukin-6 (IL-6), antioxidant enzymes (CAT, SOD and GPx), marker of oxidative stress (MDA) and blood pressure levels were investigated. Histological and ultrastructure alterations, Caspase-3 variations (immunological marker) were also investigated. The results of FT-IR showed that Zn (II) can be chelated through the carbonyl oxygen atom C=O and C–OH (Ring II) of the quercetin ligand and carbonyl oxygen atom C=O of the Art ligand forming Art/Q/Zn complex with the chemical formula $[Zn(Q)(Art)(Cl)(H_2O)_2].3H_2O$. The novel complex has a potent anti-SARS-CoV-2 activity at a very low concentration (IC_{50}=10.14 µg/ml) and without any cytotoxicity to the cellular host (CC_{50}= 208.5 µg/ml). It alleviated Acy hepatic and pulmonary toxicity by improving all biochemical markers. In conclusion, the novel formula Art/Q/Zn complex is a highly effective antioxidant agent against the oxidative stress series, and it has high inhibitory effect against the coronavirus (SARS-CoV-2).

Keywords: SARS-CoV-2; Pandemic, Artemisinin, Novel complex, SEM, TEM.

Introduction

Severe cases occurred globally essentially associated with the coronavirus's family, significantly induced by SARS-Cov-2, which caused the (COVID-19) pandemic. Despite the numerous preventive and curative measures of the recent pandemic, the novel SARS-CoV-2 continues evolving to infectious variants as recorded recently [1,2].

The reasons may be attributed to facilitating the transmission including, overcrowding defying social distancing and elevated immunodeficient population. Such situations forward

Deleted: Querctin
Deleted: † ,
Deleted: [2] ,
Deleted: [3], Reham
Deleted: Querctin
Deleted: series
Deleted: coronaviruses
Deleted: measures of
Deleted: recently[

the viral replication and increased mutation risk leading to the emergence of novel variants [3,4].

There are a few drugs that act as therapeutics for the alleviation of symptoms of COVID-19. For treatment of the viral infection, the drug should be safe, effective against viral infection and adequate for economic benefits. Coordination compounds with primary transition metal ions have gained high importance for their crucial key roles in the field of therapeutics, material sciences and biological sciences because of their availability with low cost [5]. Zinc, a vital bio-metal in nature, has excellent biological and catalytic properties making it one of the best? candidates in the field of combating against SARS-CoV-2 [6].

COVID-19 is related to a member of the family Coronavirus, SARS-CoV-2 contains main spikes [5]. Spikes play a vital role in the attachment, fusion, and entry of SARS-CoV-2 virus [6]. and this viral family has threatened human beings and it has been announced as a pandemic emergency by WHO [7]. SARS-CoV-2 contains four main proteins: spike (S), membrane (M), envelope (E) and nucleocapsid (N) proteins. Protein S plays a vital role in the attachment, fusion and entry of SARS-CoV-2 virus. S1 domains of the SARS-CoV-2 virus contain receptor-binding domains (RBD) that bind directly to the host cellular receptors [8].

Based on this understanding, therapies that directly target SARS-CoV-2 are anticipated to have the greatest effect early in the course of the disease, while immunosuppressive/anti-inflammatory therapies are likely to be more beneficial in the later stages of COVID-19 [8]. The clinical spectrum of SARS-CoV-2 infection includes asymptomatic or pre-symptomatic infection and mild, moderate, severe, and critical illness. Despite the urgent global need and world Health Organization recommendations, a therapy of COVID-19 is currently limited and includes only few drugs: remdesivir, dexamethasone, tocilizumab, ritonavir-boosted nirmatrelvir (Paxlovid), sotrovimab and molnupiravir [9]. This includes patients who do not require hospitalization or supplemental oxygen and those who have been discharged from an emergency department or a hospital [10].

SARS-CoV-2 and its variants of great concern that infects the respiratory tract, kidney, liver, heart and nervous system and may lead to series of multiple organ failure [11]. However, the recently emerged Omicron variant reduces the protective effect of vaccination and showed immune-evasive property and it is currently the dominant strain of SARS-CoV-2 around the globe [12].

Additionally, the SARS-CoV-2 surface with S1, which contains the receptor binding domain (RBD) and S2, which contains the fusion peptide. SARS-CoV can enter into the cellular host through interaction between RBD and SARS-Cov-2 and thus form 'SARS-S-RBD' with the host cellular surface through its receptor (Angiotensin-converting enzyme-2) (ACE2) as shown in Fig (1) [13,14].

The RBD of SARS-CoV 'S' protein is located in the subunit 'S1' and it is responsible for the viral binding of SARS-CoV-2 to its host cellular receptors [15, 16]. Binding of SARS-CoV-2 and ACE2 is a very critical process for pathogenesis to occur and if the binding of the virus and ACE2 receptor is blocked, the infection can be greatly stopped. Traditional medicinal plants produce compounds which are considered as active therapeutics to kill a lot of pathogens [17].

The main scientific efforts towards the discovery of new drugs to combat against SARS-CoV-2, sometimes by using computer-based methodologies that focused on targeting the main active receptors of SARS-CoV-2 such as: Mpro and ACE2 [18].

Phytochemicals were excessively studied to find potential inhibitors of Mpro via a virtual structure-based drug approach [19] reporting MD simulations and toxicity profiles of these derivatives [20].

SARS-CoV-2 infection resulted in a lot of millions of confirmed infected cases. COVID-42 pandemic affected a lot of organs of the body through induction of oxidative damage. So, an effective antiviral agent is urgently needed to combat against COVID-19 pandemic [21].

Deleted: one of the most impor
Deleted: tant
Deleted: s
Deleted: most
Deleted: Coronavirus ,SARS
Deleted: virus .
Deleted:].This
Deleted:].However
Deleted: 2 ,
Deleted: as :

Liver diseases and their complications are major health concerns for communities. They are among of the most significant causes of death worldwide. The liver is greatly affected by severe oxidative damage induced by SARS-CoV-2, owing to lack of effective treatment therapies [22].

Liver diseases include viral hepatitis, cholestasis, liver fibrosis, liver cirrhosis and primary hepatic tumours, including hepatocellular carcinoma (HCC) [23-25]. The liver is the major detoxification organ that protects against toxicity of any xenobiotic. However, it is also vulnerable to a lot of threats from the current COVID-19 pandemic and environmental xenobiotics [26].

Millions of deaths have been reported globally due to hepatic diseases and hepatitis B virus-induced liver cirrhosis was the main cause of liver-related deaths [27]. Once chronic liver disease progresses to decompensated hepatic cirrhosis, chances of effective treatment become greatly limited. Therefore, it is of great importance to explore alternative effective drugs, especially given the progressive prevalence of hepatic dysfunction diseases.

Artemisia annua L. is effective in the treatment of malaria, antimicrobial activities, hyperlipidemia and inflammatory diseases and has a good safety record [28].

Artemisinin (Art) is *(Artemisia annua* L.*)* derivative and it belongs to a family of drugs approved for the treatment of malaria with known clinical efficacy. Additionally, Art displays anti-viral and anti-cancer effects. Recently, much more attention has been paid to the miracle key role of artemisinin in treatment of hepatic diseases. Recently, several studies suggested that Art can protect the hepatic tissues from different hepatic dysfunction as proliferation and metastasis [28].

Artemisia annua L. has a beneficial and safety record in the treatment of malaria, antimicrobial activities, hyperlipidemia and inflammatory diseases [28].

Artemisinin (Art) which is an active ingredient, it has an excellent low toxicity, safety profile and is relatively cheap. Additionally, these drugs have potential and effective properties. Art can be used either alone or combined with other drugs to elevate its therapeutic effectiveness and share essentially in the retardation of cases of drug resistance [28]. Thus, world need discovery of new antiviral drugs and an effective strategy to treat emerging diseases that could be trusted safely.

Acrylamide (Acy) is found in starchy foods that had been heated over long periods over 120 °C [29]. Acy is formed in the Maillard reaction, non-enzymatic glycation of proteins [30]. This reaction occurs between the amine group residue (-NH_2) of proteins and the carbonyl group (C=O) from carbohydrates when food is heated above 120°C.

Acy isn't a food additive, but it is a by-product of the cooking processes and could be produced when the food is cooked at very high temperatures. Acy was classified as a Group 2A carcinogen by the international Agency for Research on carcinogens, In previous experimental rat models, Acy led to testicular tumors [31,32], hepatotoxicity [33] and lung toxicity [31].

Nowadays, hepatic disorders are facing serious side effects. So, it is necessary to seek for new safe medicines for the liver diseases especially, those originating from natural resources [34].

Quercetin (Q) is a natural flavonoid occurring widely in plants and shows many benefits such as antioxidant and anti-inflammatory activities. Additionally, Q administration minimizes the oxidative damage. Q supplementation is a vital in normalizing blood glucose levels and reducing serum cholesterol levels. Additionally, Q improves antioxidant capacities and prevents oxidative injury [35].

Q protects and alleviates against inflammatory storms [36], particularly from the viral infections. Nutrients promote the immune response. The role of micronutrients, such as Zn, in treating many inflammatory diseases has been extensively evaluated [37].

There is a strong correlation between Zinc levels and organ dysfunction based on the association between many diseases and Zn transporter polymorphisms via the ZnT8 gene [38]. Zn plays a vital role in treating pulmonary diseases [39]. Zn supplementation inhibits pneumonia, and it can increase resistance against infections [40].

Deleted: ingredient ,

Deleted:].This

Deleted: additive

Deleted:] ,

Deleted: pneumonia

Our previous study revealed that synthesised ZnO-NPs have inhibitory activity against SARS-CoV-2 when it is used as a nano-spray against SARS-CoV-2 infection but with some cytotoxic activity [42].

Please, also cite your work from Heliyon,. The differences between this and that paper can and should be included in the discussion too! This improves transparency!

The current study is designed to characterise the spectroscopic and chemical structure of a novel synthesised Art/Q/Zn complex, to evaluate its cytotoxicity and antiviral activity against SARS-CoV-2 and to assess its antioxidant capacities, alleviation of hepatotoxicity and pulmonary toxicity induced by Acy in male rats.

2. Materials and Methods

2.1. Ethical Approval

The inhibitory effect of the novel Art/Q/Zn complex against SARS-CoV-2 was tested at the Centre of Scientific Excellence for Influenza Viruses, National Research Centre, Dokki, Egypt using the SARS-CoV-2 isolate hCoV-19/Egypt/NRC-03/2020 (GSAID Accession Number: EPI-ISL-430820). The biological activity of the novel complex was tested on male rats according to the ethical approval committee of Zagazig University, approval number ZU-IACUC/2/F/61/2022. This study was also sanctioned by the Taif University ethical committee, accredited by the national committee for Bioethics under No. HAO-02-T-105. The SARS-CoV-2 strain sample used in the research has ethical approval and the accession number: hCoV-19/Egypt/NRC-03/2020 (Accession Number on GSAID: EPI_ISL_430820). The bio-sample's record history can be accessed through the link: https://www.ebi.ac.uk/biosamples/samples/SAMN14814607. The available phylogenetic analysis is accessible at: http://purl.obolibrary.org/obo/NCBITaxon_2697049.

(https://www.ebi.ac.uk/ols/ontologies/NCBITAXON/terms?iri=http%3A%2F%2Fpurl.obolibrary.org%2Fobo%2FNCBITaxon_2697049). – and this is?

2.2. Chemicals and instrumental Analyses

Quercetin (Q) (Fig. 2A), Artemisinin (Art) (Fig.2B), Zinc chloride ($ZnCl_2$) and Acrylamide (Acy) were obtained from Sigma-Aldrich, USA (products reference / cat#?), and used without undergoing purification. The analytical instruments employed are registered in Table 1.

2.3. Synthesis of the mixed ligand zinc complex

The Art/Q/Zn complex was prepared according to the following procedure: an ethanolic solution of zinc chloride (1 ml mole, 0.137 g – What's this? 0.1M solution?), was mixed with an ethanolic solution of Q (1 m mole, 0.302 g What's this? 0.1M solution?),) and an ethanolic solution of Art (1ml mole, 0.283 g What's this? 0.1M solution?),). They were further diluted (?) in 25 ml of ethanol (making a final concentration of?). The pH was adjusted to 8-9 using 10% ammonia solution. The solution was refluxed for 5h using??? before filtration (with?? Filter pore?) and washing with ethanol (%?) and distilled water (ultrapure?). Finally, the resulting solid mixed ligand complex was dried in a desiccator (Fig.2, 3). Figure 2., why??

Temp conditions? Light/dark conditions?

Looking at fig. 3, this description can and should be improved!

2.4. Cytotoxicity assay

To evaluate the maximal half cytotoxic concentration (CC_{50}) of the newly synthesized complex 140 why 140?!) (Art/Q/Zn), a stock solution of Art/Q/Zn was prepared using a 10%

Formatted: Highlight
Deleted: on
Deleted: (
Deleted:)
Deleted: (
Deleted:),
Deleted: (
Deleted:) and was also approved
Deleted: that is
Deleted: with
Deleted: Strain of t
Formatted: No underline
Deleted: with
Deleted: (
Deleted: link of the
Deleted: bio-sample with record history
Deleted: With
Formatted: No underline
Formatted: No underline
Formatted: Highlight
Deleted: 2 a,b
Formatted: Highlight
Deleted: provided by
Deleted: ‘
Deleted: ’
Formatted: Highlight
Deleted: analyses tools are shown
Deleted: .
Deleted: .
Deleted: E
Deleted: s
Deleted: were
Formatted: Highlight
Deleted: before they were dissolved
Formatted: Highlight
Formatted: Highlight
Deleted:
Formatted: Highlight
Formatted: Highlight
Formatted: Strikethrough
Formatted: Highlight
Deleted: novel
Deleted: (Art/Q/Zn)
Formatted: Highlight

mixture of DMSO, diluted with DMEM and di-distilled water. The cytotoxic activity of Art/Q/Zn was tested on VERO-E6 cells by using the MTT assay 142 as previously described in our previous study [42]. Briefly, VERO-E6 cells were seeded in 100 µl/well and then incubated at 37 °C and CO_2 for about 24 h. 144 After one day, VERO-E6 cells were treated with different concentrations of Art/Q/Zn and tested in 145 triplicates. Then, the supernatants were discarded, and the monolayers were washed with MTT solution (5 mg/mL of Art/Q/Zn solution) beside sterile phosphate buffer saline for 3 times and 147 incubated at 37 °C for 4 h. The well-formed formazan crystals were dissolved in 200 µl of isopropanol mixed with HCl. Formazan crystals absorbance was measured at range between 540 and 149 620 nm using a multi-well plate reader. The % of cytotoxicity was determined by the following equation:

% Cytotoxicity = (absorbance of cells without Art/Q/Zn (Control) –absorbance of cells with Art/Q/Zn) X 100 / absorbance of cells without Art/Q/Zn.

It appears a copy-paste with line numbers here, gone wrong? Additionally, the language should sound like: "VERO-E6 cells were seeded at a volume of 100 µl per well and incubated at 37°C in a CO2 environment for approximately 24 hours. Following this, varying concentrations of Art/Q/Zn were administered to the VERO-E6 cells in triplicates. Subsequently, the supernatants were discarded, and the cell monolayers underwent three washes using MTT solution (5 mg/mL of Art/Q/Zn solution) in combination with sterile phosphate buffer saline. The cells were then incubated at 37°C for 4 hours.

The resultant formazan crystals were dissolved in a mixture of 200 µl of isopropanol and HCl. The absorbance of the formazan crystals was measured within the wavelength range of 540 to 620 nm, using a multi-well plate reader. The calculation of cytotoxicity percentage was performed according to the equation:"

2.5. Determination of Inhibitory Concentration 50% (IC_{50})

In well plates for tissue cultures, Vero-E6 cells were well distributed and then, they were incubated at (37 °C under CO_2) overnight. The cellular monolayers were washed three times with phosphate buffer and then exposed to virus adsorption (hCoV-19/Egypt/NRC-03/2020 (Accession Number on GSAID: EPI_ISL_430820)) for 1 hr at room temperature (RT). At 37 °C for only 1 hr The monolayers were overlaid with DMEM media which containing concentrations of Art/Q/Zn. After incubation at 37 °C for 72 h, VERO-E6 cells were treated with paraformaldehyde that was freshly prepared as (4% paraformaldehyde/PBS), just warming PBS (Phosphate buffer saline) then, with continuous vigorous stirring, slowly add paraformaldehyde, then gradually add a few drops of 0.1 M NaOH based on [41] that confirmed that paraformaldehyde dissolved in fixed alkali hydroxide solution , then filter with filter paper till obtain solution with pH 7.9 for 20 minutes at room temperature and stained with 0.1% crystal violet stain in distilled water for about 15 minutes. Then, we add methanol for each well for dissolving the crystal violet dye and the color optical intensity of Art/Q/Zn was measured at 570 nm by using multi plate reader. The IC_{50} of Art/Q/Zn is needed to decline the "SARS-CoV-2" cytopathic effect by 50% percentage, which is relative to control SRAS-CoV-2 [41].

2.6. Animal treated groups and animal ethics approval

The animals were treated in accordance with the ethical approval committee of both Zagazig and Taif University under ethical approval numbers: (ZU-IACUC/2/F/61/2022) and (HAO-02-T-105). Male rats weighing between 150 and 180 g were obtained from the animal house of the Faculty of Pharmacy, Zagazig University. Healthy animals aged 6-weeks and free of any pathogen were kept at the animal house of the Zoology Department (Physiology division) at the Faculty of Science. The animals were placed under standard laboratory conditions (27 °C and a normal daylight cycle). Food and water were provided *ad libitum*. The experiment was carried out on 40 male rats, randomly divided into four groups The rats were administered the treatments orally (By using oral gastric tube) for 30 days as follows:

Deleted: in 10% with mix of DMSO, diluted with DMEM and 141 di-dist. Water. The cytotoxic activity of Art/Q/Zn was teste
Formatted: Highlight
Deleted: (
Deleted:)
Formatted: Highlight
Formatted: Highlight
Formatted: Highlight
Formatted: Highlight
Deleted: .
Formatted: Indent: First line: 0 cm
Formatted: Indent: Left: 0 cm, First line: 0 cm
Formatted: Indent: First line: 0 cm
Deleted: (37
Deleted: were washed
Deleted: Then ,
Deleted: "
Deleted: "

Group I: control group: the animals received normal physiological saline (0.9% NaCl).
Group II: was administrated Acy at a dose of 500 mg kg^{-1} in saline solution [33].
Group III: was administered with Art/Q/Zn at a dose of 30 mg Kg^{-1} and dissolved in normal physiological saline [35].

Group VI: was orally given Acy the Art/Q/Zn complex after 30 min, as described previously with the same treatment and the same doses (Fig. 4,5) for 30 successive days.

2.7. Samples collection

Blood samples were centrifuged at 5000 r.p.m for about 5 minutes to obtain the serum, The serum was used for further analysis, and it was persevered at -20°C. The experimental male rats were suddenly decapitated after light anesthesia with xylene/ketamine (I.P), and both the liver and lung tissues were removed, 1st part was used for histological, ultra-structural and immune testing, Meanwhile the 2nd part was weighed, and homogenized and used for evaluation of antioxidant enzyme capacities (Fig.1). The supernatants of tissue homogenates were obtained after centrifugation at 3000 g for 15 minutes at 4°C, then the supernatants were collected and preserved at -20 °C for future analysis.

2.8. Biochemical investigation

2.8.1. Measurement of hepatic functions and inflammation markers

After successive 30 days of treatment, some biochemical markers in serum were assessed as the activity of alanine aminotransferase (ALT), aspartate aminotransferase (AST) by using available commercial kits from (Spinreact Co, Spain) according to the instructions. Serum LDH activity was assessed by using LDH kit (GmbH Schigraben, Hannover, Germany).

The ELISA technique was conducted (Ebio-Science) by following the instructions to determine tumor necrosis factor-alpha (TNF-α), interleukin-6 (IL-6) and determination of (CRP) C-reactive protein.

2.8.2. Assessment of oxidative stress markers

A small piece (0.25 g) of the hepatic tissues were homogenized with cold buffer and it was centrifuged to get the supernatant that was further used for performing antioxidant assays. According to Ohkawa et al. [43], malondialdehyde (MDA) was measured.

Superoxide dismutase enzyme activity (SOD) was assessed according to Sun et al. [44], CAT activity was estimated according to Aebi, and the breakdown rate of hydrogen peroxide was at 240 nm (Spectrophotometer SP-2200, Bioespectro) [45], it was expressed in (U/g). Glutathione peroxidase (GPx) activity was estimated according to the manufacturer instructions [46].

2.9. Histological and immunohistochemically assessment of both liver and lung tissues

Fixed samples were processed by using hematoxylin/eosin staining of liver and lung tissue sections. Photomicrographs of the tissue samples were taken by light microscope to view the stained slides. The excessed liver and lung slices (4 mm thickness) were blocked with 0.1% mix of water and methanol for 1/4 h to study apoptosis-related proteins. After the blocking process, both tissue sections were treated at 4°C overnight with polyclonal caspase-3 antibody. The color intensity of caspase-3 in the immunohistochemical sections was used to classify the intensity as the following: (+) means (weak immunoreactivity), (++) means (moderate immunoreactivity), (+++) means (High and strong immunoreactivity), and (++++) means (very high immunoreactivity).

2.10. Measurement of blood pressure (BP)

Systolic, diastolic and mean arterial blood pressures were measured on 18thday pregnancy, using noninvasive BP measurement system (NIBP 250, Serial No: 21202-108, BIOPAC system, Inc.; USA) [47].

Deleted: I :
Deleted: group :
Deleted: analysis
Deleted: 1.Measurment
Deleted: of hepatic
Deleted: the instructions
Deleted: of oxidative
Deleted: activity(
Deleted: SOD) was
Deleted:],.
Deleted: Aebi
Deleted: following :

2.11. Molecular docking, Physicochemical, and pharmacokinetics studies

Here in the study, analyzed the pharmacophoric features of SARS-CoV ACE2 receptor co-crystallized inhibitor (Art/Zn) to synthesize novel compounds using the ligand-based design approach [48]. We synthesized a novel Art/Zn formula that can bind with ACE2 receptors that bind SARS-CoV-2.

Generalized molecular mechanics during molecular docking simulations of complex. We used Swiss dock tool and referenced study [49].

2.12. Statistical and data analysis

The data were expressed as mean ± SE., a One-Way Analysis of Variance was employed for comparing several groups, using post-hoc test. Statistical significance at $P \leq 0.05$ [50]. We assumed that CAT in hepatic tissue homogenates in Acy group versus Acy+ Art/Q/Zn group are 2.49 ± 0.86 versus 4.21 ± 0.95 (U/g). At power 80% and confidence level 95%, sample size is 40 (10 in every group). This sample was calculated by OPEN EPI software package [50].

3.RESULTS

3.1. Physical measurements data

The zinc chloride salt reacted with the mixed ligands of artemisinin and quercetin according to the following equation: $ZnCl_2$+ artemisinin (Art) + quercetin(Q) = $[Zn(Q)(Art)(Cl)(H_2O)_2].3H_2O$

The proposed structure for zinc mixed ligand complex $[Zn (Q)(Art)(Cl)(H_2O)_2].3H_2O$ (Molecular formula: ($C_{30}H_{41}O_{19}ClZn$)) was in (Fig.6) and elemental analysis value: (%C= 44.72 , %H=5.09 , %Cl=4.40) which shows that the molar reaction ratio is 1:1:1 for Zn :Q : Art .The new zinc complex was soluble in DMSO and stable in air. Molar conductivity value (Λ_m) was 23 $ohm^{-1}.cm^2.mol^{-1}$, confirming the non-electrolytic nature of the mixed ligand complex [51].

3.2 Infrared spectra

Infrared for Quercetin (Q), Artemisinin (Art) and their zin complexity are shown in Fig.7 the assignments for main vibrational bands:

For free ligand (Quercetin) broad strong bands appear at 3563 and 3388 cm^{-1} referring to stretching vibration of hydroxyl (OH) for poly phenolic groups. For Q with Zn(II) there is strong broad band appeared at 3372 cm^{-1} referring to molecules of water, which is convenient with the suggested structure (Fig.6) of mixed ligand complex $[Zn(Q)(Art)(Cl)(H_2O)_2].3H_2O$. Also, for free (Q), the ν(C4=O) stretching vibration of carbonyl group appeared at 1679 cm^{-1}, while for $[Zn(Q)(Art)(Cl)(H_2O)_2].3H_2O$ complexity, occur shifting for this band in the range 1613-1660 cm^{-1}. This confirmed that Zn (II) can be chelated through the carbonyl oxygen atom C (4)=O and C(3)–OH of the (Q) ligand [52]. Stretching vibration band for ν(COC) of ether group in the ring II for (Q) is appeared at 1269 cm^{-1}, where no shift occur for this band after chelation, also ν(COC) of ether group in the ring of Art is appeared at 1260 cm^{-1} and no shift occur for this band after chelation which confirm that this band is not involved in coordination. The ν(C–OH) for free (Q) appears at 1409 cm^{-1}, where occur shifting from 1361-1383 cm^{-1} for $[Zn(Q)(Art)(Cl)(H_2O)_2].3H_2O$ complexity and this confirm the involvement of C(3)–OH phenolic oxygen group (ring II) in chelation process.

For Art free ligand, many broad strong bands appeared at 3752 and 3692 cm^{-1} referring to ν(O–H) of formed O---H hydrogen bond between hydrogen atom and oxygen atom of the ring. Also, for free Art, the ν(C=O) stretching vibration of carbonyl group appeared at 1736,1689 cm^{-1}, while for $[Zn(Q)(Art)(Cl)(H_2O)_2].3H_2O$ complexity, occur shifting for this band in the range 1652-1722 cm^{-1}. Confirming that Zn (II) can be bonded via carbonyl (O)

Deleted: w
Deleted: synthesizing
Deleted: formula
Deleted:].We
Deleted: H_2O (
Deleted: appeared at
Deleted: 3372
Deleted: of water
Deleted: Also
Deleted: band after
Deleted: in coordination
Deleted: ^{1},where
Deleted: Also
Deleted: binded

atom C=O of the Art ligand. Stretching vibration bands for ν(C-H) aliphatic are appeared at the range 2851-2967 cm^{-1}, for Art free ligand and $[Zn(Q)(Art)(Cl)(H_2O)_2].3H_2O$ complex.

For Art, the stretching vibration band for ν(COC) of ether group is appeared at 1260 cm^{-1}, where no shift occur for this band after chelation which confirm that this band is not involved in coordination. The $[Zn(Q)(Art)(Cl)(H_2O)_2].3H_2O$ has new bands appeared within wavenumbers 611–645 cm^{-1}, that are referring to stretching vibration for zinc-chloride bond [43,44].The bands appeared at the range 497-511 and 473 -449 cm^{-1} are referring to ν(Zinc–O), the stretching vibration which confirm the formation of metal complexity [53].

Deleted: for ν

Deleted: ^{1},where

Deleted: shift occur

Deleted: in coordination

Deleted: H_2O has

3.3. UV–Vis spectra and magnetic data

The UV–Vis spectrum of the quercetin free ligand has absorption bands observed at 290 and 365nm assigned to π→π* and n→π* transitions while Art free ligand has three absorption bands observed at 295 and 354 nm assigned to π→π* and n→π* transitions respectively [54]. The electronic absorption spectra for Zn (Q)(Art)(Cl)$(H_2O)2].3H_2O$ complex has two absorption bands at 290nm and 345 nm due to π→π* and n→π* electronic transitions respectively (Fig.8) and (Table. 2) and considered as diamagnetic. Due to complexing formation caused by conjugated system by complexation that make bathochromic shift [55]. For zinc mixed ligand other bands are appeared at 415 nm, 440 nm and 455 nm these bands can be due to M→L charge transfer transition. The magnetic moment value obtained for Zn (III) complex lies at 3.98 BM which corresponds to the octahedral field.

Deleted: nm and

3.4. ^{1}H-NMR spectra

^{1}H-NMR spectrum for free Q ligand shows the following signals: (1H, C5-OH) : δ 12.52, (1H, C7-OH) :10.80, (1H, 3-OH): 9.54,(1H, 4′-OH): 9.61, (1H, 3′-OH) :9.32, (1H, 2′-H): 7.62 , (1H, 6′-H) :7.54 ,(1H, 5′-H) : 6.89,(1H, 8-H) :6.37, (1H, 6-H):6.15 [56]. For mixed ligand complex $[Zn(Q)(Art)(Cl)(H_2O)_2].3H_2O$ (Fig.9) the main signal bands appeared are : (1H,5-OH) :δ 12.492, (1H, 7-OH) :10.806, (1H, 4′-OH) :9.67, (1H, 3′-OH) :9.383, (1H, 2′-H) :7.664, (1H, 6′-H) 7.661, (1H, 5′-H) : 7.534,7.521, (1H, 8-H)6.874, (1H, 6-H) :6.856, 6.390, 6.387 . According to these data, the band appears at δ 9.54 for free Q assigned to (1H, 3-OH) disappears for $[Zn(Q)(Art)(Cl)(H_2O)_2].3H_2O$ and other signal bands not shifted, confirming that hydroxyl group at C-3OH is deprotonated and involved in coordination with Zn(II) also there is a new signal band appeared at δ 3.335 ppm for $[Zn(Q)(Art)(Cl)(H_2O)_2].3H_2O$ which is assigned to protons of H_2O coordinated and uncoordinated. Based on the above data the complexation structure for $[Zn(Q)(Art)(Cl)(H_2O)_2].3H_2O$ was confirmed.

3.5. X-ray diffraction (XRD) analysis

X-ray powder diffraction patterns used to determine the crystallinity of zinc mixed ligand complex at the value of (2θ) 4–80◦ and also used to examine the nano structural form for zinc mixed ligand complex. X-ray diffractogram of [Zn (Q)(Art)(Cl)$(H_2O)_2].3H_2O$. According to x-ray diffraction pattern, a broad peak at 2θ = 23° appeared, suggesting that zinc mixed ligand complex has amorphous structure [57] as shown in Fig.10. All our attempts to prepare single crystals were failed.

Deleted: ° appeared

Deleted: ,

3.6. Scanning electron microscopy SEM and EDX

The technique of SEM is used to determine the physical and microscopic character of [Zn(Q)(Art)(Cl) $(H_2O)_2$].$3H_2O$ that is shown in Fig. 11. SEM can be taken as indication for the presence of a single component for [Zn(Q)(Art)(Cl) $(H_2O)_2$]. $3H_2O$.The images of [Zn(Q)(Art)(Cl)$(H_2O)_2$].$3H_2O$ clarify a small particle size with a Nano-feature products. The surface morphology of Zn (II) mixed ligand complex was checked using SEM which showed a small particle accompanied with a high ability to agglomerates formation with different shapes and EDX clarified the elemental analysis of the novel complex with percentage (Fig 12).

3.7. Transmission electron microscopy TEM

The TEM images for synthesized [Zn(Q)(Art)(Cl)$(H_2O)_2$].$3H_2O$ complex is in Fig.13. The uniform matrix for [Zn(Q)(Art)(Cl)$(H_2O)_2$].$3H_2O$ complex was cleared in the pictograph and this confirms that [Zn(Q)(Art)(Cl)$(H2O)_2$].$3H_2O$ complex has a homogeneous phase where spherical black spots like shape is observed for Zn(II) complex with the particle has size ranged of 31.99-48.13 nm.

Deleted: where spherical

Deleted: for Zn

Deleted: particle has

3.8. Cytotoxicity Assay

Art/Q/Zn novel complex showed high inhibitory activity against SARS-CoV-2 in very low concentration (IC_{50}=10.14 µg/ml). This assay was used to assess the possible cellular cytotoxicity of Art/Q/Zn that was (CC50=208.5 µg/ml) (Fig.14) and attached image for crystal violet analysis with silver crystals formed and successive dilution and appearance of high antiviral activity of Art/Q/Zn by appearance of pale purple color that indicate inhibition of SARS-CoV-2 cells growth.

3.9. Biochemical evaluation

Table.3 and Fig.S1 showed the serum enzyme activities of AST, ALT and LDH that were significantly elevated in Acy treated group more than control group. The current findings indicated that the cellular membrane disruption mainly occurred. Meanwhile, Art/Q/Zn mixed ligand novel complex with dose 30 mg/kg was evaluated to be normal for the enzyme activity of hepatic functions. A decline in the hepatic enzymatic activities were recorded after treatment with Art/Q/Zn after Acy was administration to male rats.

CRP, IL-6, and TNF-α levels were significantly higher in Acy treated group compared with the control group (Table 4). The levels of CRP, IL-6, and TNF-α were significantly lower in Art/Q/Zn either alone or after Acy administration compared to Acy treated group only (Table 4).

Table.5 showed that antioxidant enzymes levels were significantly declined as a result of treatment with Acy.as it reduced CAT, SOD, and GPx activities significantly. Acy treated group had greater levels of MDA in the hepatic tissues more than the control group. Acy afforded oxidative injury in the liver tissues homogenates of male rats, which is an indicator of an increment of oxidative injury with decline in the antioxidant enzyme levels (Table.5).

3.10. Histological and ultrastructural examination of liver and lung tissues (Histological, TEM and immunostaining sections) with live sections clarifying variations in structure of studied tissues

After administration of Acy and Art/Q/Zn, hepatic tissues showed toxicity in the form of fatty change with marked and elevated of the hepatocytes' degeneration and showed congested portal vein with hemorrhage inside it and infiltration of blood sinusoids by mononuclear inflammatory cells (Fig.15). The liver, after administration of Acy and Art/Q/Zn, showed alleviation of hepatotoxicity with restoration of normal hepatic tissues (Fig. 15).

TEM examination of hepatic tissues showed normal structure in both control group and Art/Q/Zn treated group with normal nucleus with nuclear boundaries, normal-sized mitochondria and endoplasmic reticulum. Meanwhile, Acy treated group showed detaching of hepatic structures and pyknosis of nuclei with dysregulation of nuclear boundaries and restoration of normal hepatic structure in group treated with Acy and Art/Q/Zn as it alleviated the hepatotoxicity (Fig.16).

Immunostaining of the hepatic tissues showed high immunoreactivity for caspase-3 in hepatic tissues in group treated with Acy. Meanwhile, the immunoreactivity for caspase-3 was very weak in the group treated with Acy and followed by Art/Q/Zn as shown in (Fig.17).

After administration of Acy and Art/Q/Zn, rat lung tissues showed toxicity in the form of (Fig.18). The lung tissues, after administration of Acy and Art/Q/Zn, showed alleviation of pulmonary fibrosis with restoration of normal pulmonary tissues (Fig. 18).

TEM of lung tissues examination showed normal structure in both control group and Art/Q/Zn treated group with normal nucleus, normal basement lamina, alveolar sacculus and normal Bronchioles. Meanwhile, Acy treated group showed large red blood cells that block completely the air sacs with appearance of small granules with detaching of most pulmonary tissues with pulmonary fibrosis. Meanwhile, restoration of normal pulmonary sacculus and alveolar epithelial cells in group treated with Acy and Art/Q/Zn as it alleviated the lung fibrosis and hemorrhage (Fig.19).

Immunostaining of the pulmonary tissues showed high immunoreactivity for caspase-3 in group treated with Acy. Meanwhile, the immunoreactivity for caspase-3 was very weak in the group treated with Acy and followed by Art/Q/Zn as shown in (Fig.20).

Fig.21 showing the different morphological variations in both lung and liver tissues of either Acy or Art/Q/Zn as Liver of Acy group showed hepatomegaly, dark oxidative color and some lesions, Also, lung tissues of Acy treated group showing large lesions with congested tissues and hemorrhage. On the other hand, the liver and lung tissues of normal appearance with bright red color and without any lesions or structural changes.

3.11. Effect of Art/Q/Zn on blood pressure levels

Control group showed normal heart rate with normal blood pressure recorded by systolic pressure 134.9 mmHG, diastolic pressure 108.7 mmHG and heart rate 263.2 beats/min (bpm) (Fig.22A). Acy induced elevation in systolic and diastolic blood pressure by 188.20 mmHG and 162.02 mmHG, respectively with slightly higher heart rate recorded as 297.0 beats/min (bpm) than that of the control group (Fig.22 B). The Art/Q/Zn complex caused a significant reduction in systolic pressure than control group and Acy group recorded as 102.05 mmHG and diastolic blood pressure as 82.94 mmHG after 30 days of treatment but with a significant increment in heart rate by 379.78 beats/min (bpm) (Fig.22C). However, treatment of male rats with a combination of Acy followed by the Art/Q/Zn complex induced a more pronounced reduction in systolic and diastolic blood pressures (by 134.95 and 263.54 mmHG) than in the Acy-only treated group with the lowering of heart rate recorded as (263.54 beats/min) (bpm) (Figs 22D), All measurements for systolic and diastolic blood pressure with recording heart rate for all treated groups were carried out by digital blood pressure measurement system (NIBP250), BIOPAC systems, inc., and values were measured in rats after putting in the streamer (Fig.22E). Systolic and diastolic values were shown in both (Fig.S2 and Table 6).

3.12. Molecular docking studies

In the initial phase of the docking process, the programme was set up by redocking the formula (Art/Q/Zn) against angiotensin-converting enzyme-2 (ACE2) and this receptor may generate a protective effect in the COVID-19 patients by reduction of the severe respiratory symptoms risk and M^{pro} target main protease for SARS-CoV-2 and it is the key enzyme of coronaviruses and has a key vital role in mediating viral replication and transcription, as shown in Fig.23 (A) (v1-v6). Also, Lipophilicity capacities were shown as most therapeutics essentially used speciliazed transport systems of the body and mostly instead of that mechanicm , others tend to

Deleted: (

Deleted:).The

Deleted: tissues ,

Deleted: sacuulus

Deleted: imunoreactivity

Deleted: bpm) than

diffuse via the cellular membrane. To do so, therpautics must be suffieciently lipophilic. So, If therpaeutics showed lipophilicity affinity , this enable easy cellular diffusuion and thus getting much better effect of the therapeutics used and Fig.23 showed high lipophilicity capacities of novel synthesized complex (Art/Q/Zn) with both SARS-CoV-2 receptoes (ACE2) Fig. 23 (B) and main SARS-CoV-2 inhibitor (M^{Pro}) Fig.23 (C).

3.13. Molecular dynamics (MD) simulation

Molecular dynamics (MD) simulations were performed for Art/Q/Zn at (100 ns) by using Desmond, a Package of Schrödinger Fig.23 (A).MD Simulations were carried out to predict the ligand binding status in the physiological environment to mimic the predicted binding of the novel complex (Art/Q/Zn) with the main receptors of ACE2 and M^{Pro} (The main protease of SARS-CoV-2) (Fig 23 (B and C)).

3.14. Histogram and heat map analyses

Histograms were described in (Fig.24 (A1 and B1))and heat maps as shown in (Fig.24 (A2 and B2) for the SARS-CoV-2 ligand-protein of Art/Q/Zn complex with ACE2 and M^{Pro}, respectivley during the simulation time (100 ns).

3.15. Ligand properties

Regarding Art/Q/Zn complex with ACE2 (Fig.24 (A3)), GLN-72 contributed about 99%, besides GLN-59 contributed about 49% followed by LYS-51, LEU-54 and PHE-55 contributed as follows respectively (41,66, 41,38 and 31%) of the interactions as H-bonding; However, ILE-61 , VAL-93 , ILE-19 and MET-62 formed mainly the hydrophobic interactions. Additonally, LYS-51, LEU-54, PHE-55, GLN-59 and GLN-72 were the main members contributing to the water-bridges, with no ionic bonds were recorded. Obviously, GLN-72 was the most participating amino acid in the interactions through hydrogen bonds.

By analysing the docking results for our synthesized complex against ACE2 and M^{pro} receptors of SARS-CoV-2, we can conclude that the Protein-Ligand contact as follows: the redocked cocrystallised formula formed hydrogen bonds in case of ACE2 with GLN-18,ILE-19,GLN-24,LYS-51,LEU-54,PHE-55,LEU-57, GLY-58, GLN-59, ILE-61, MET-62, TYR-67,GLN-72, VAL-75, VAL-93, LYS-94, HIS-96 and TYR-100 incase of ACE2 receptor (Fig.24 (A3)) and PHE-8, LYS-102, VAL-104, ARG-105, ILE-106, GLN-107,GLY-109,GLN-110, THR-111, ASN-151, ILE-152, ASP-153, TYR-154, CYS-156, SER-158, CYS-160, ASN-203, ASP-248, THR-292, PHE-294, ASP-295, ARG-298 and GLN-306 incase of M^{Pro} with a very high activity and the Art/Q/Zn complex showed a binding interaction energy as shown in (Fig.24 (B3)).

Additionally, for the SARS-CoV-2 ligand-protein of Art/Q/Zn complex with M^{pro} during the simulation time (100 ns) are described in (Fig.24-B3). Regarding Art/Q/Zn complex with M^{Pro}, GLN-10 contributed about 99%, besides PHE-8 contributed about 60% followed by ASP-298 and THR-111 contributed as follows respectively (58 and 57 %) of the interactions as H-bonding; However, PHE 294 and LYS-102 formed mainly the hydrophobic interactions. Additonally, ASP-248 , THR-111, CYS-156 and GLN-110 were the main members contributing to the water-bridges, with ionic bonds were recorded in both ILE-152 and ARG-298.Obviously, GLN-10 was the most participating amino acid in the interactions through hydrogen bonds.

3.16. RMSD analysis

The RMSD values of Cα atoms were evaluated for Art/Q/Zn complex to monitor the effect of this novel complex on the conformational stability of ACE2 and M^{pro} receptors during the simulations. The results as seen in (Fig. 24- A4 and B4). The fluctuation of the proteins was within acceptable variation with RMSD values of less than 2.00° A incase of ACE2 and less than 3.00°A incase of M^{Pro}, indicating the stability of the protein conformation.

Ligand features, including the RMSD, radius of gyration (rGyr), solvent accessible surface area (SASA), the, intramolecular hydrogen bond (intraHB), molecular surface area (MolSA), and polar surface area (PSA), are showed in Fig.24 (A4 and B4). Other ligand properties are reported in the root mean square deviation (RMSD).

The RMSD and rGyr for Art/Q/Zn complex with ACE2 were observed to be within the range of (0.7–1.9) Å. Also, with no intraHB bands were observed during the 100 ns of simulation and the MolSA range was within (65–512 Å2). Additionally, the SASA was within the (35–400 Å2), Moreover, its PSA range was between 10 and 130 Å2 (Fig.24 (A4)).

The RMSD and rGyr for Art/Q/Zn complex with M^{Pro} were observed within the range of (0.3–2.6) Å, respectively. Also, intraHB with bands were observed rang to~2 during the 100 ns of simulation and the MolSA range was within (70–285 Å2). Additionally, the SASA was within the (80–320 Å2) Moreover, its PSA range was between 25 and 260 Å2 (Fig.24 (B4)).

The ligand properties showed fluctuation and torsion at the beginning of the simulation (Fig.24 A5 and B5) before reaching equilibrium, indicating the stability of Art/Zn complex to the active site of the SARS-CoV-2 main protease active sites.

4. Discussion

The COVID -19 pandemic is a serious global challenge which has altered the global economic health. Thus, we need to repurpose recently discovered active compounds and combine them with drugs to obtain novel formula to increase the therapeutic effectiveness of active compounds for enhancing their effectiveness against resistant strains of bacteria or viruses.

This study aimed to characterise a novel synthesised metal complex (Art/Q/Zn) for its chemical structures and antiviral activity against SARS-CoV-2 *in vitro*. Both IC50 and CC50, antioxidant capacities and physiological, histological and ultra-structural effects on both liver and lung against toxicity induced by Acy were tested *in vivo* in male rats. Our findings confirmed the novelty of the Art/Q/Zn chemical structure and confirmed its high activity against SARS-CoV-2. The Art/Q/Zn complex also exhibited high antioxidant activities against oxidative stress induced by Acy and improved the physiological functions of both the liver and lung. It also alleviated any structural alterations induced by Acy, especially for pulmonary tissues. It also restored normal alveolar sacs, normal hepatic architecture and expressed negative to mild immunoreactivity against Caspase-3 immunostaining with declining inflammatory markers.

Deleted: z

Additionally, the novel complex helped in lowering high blood pressure induced by Acy, highlighting its potential activity on renal physiological functions. The findings also confirmed the complex has a positive effect on angiotensin-converting enzyme 2 (ACE_2) receptor, which is an enzyme that can be found attached to the cellular membrane of the intestines, kidney, testis, gallbladder and heart or in a soluble form and plays a vital role in keeping the body's blood pressure in a normal range. The complex is vital in order for the enzyme ADAM17 to cleave its extracellular domain to create soluble ACE_2. Soluble ACE_2 lowers blood pressure by catalysing the hydrolysis of angiotensin

II (a vasoconstrictor peptide) into angiotensin (1–7) (a vasodilator) [58,28] which in turns binds to MasR receptors creating vasodilation and hence decreasing blood pressure [59]. This decline in blood pressure makes the entire process a promising drug target for treating hypertension and cardiovascular diseases [60,61]. Thus, this receptor plays a vital role in hypertension drugs and thus maintains renal function and its reabsorption abilities.

Art, with other active compounds or metals, can be used to elevate therapeutic effectiveness of its characteristics and inhibit the progress of any drug resistance. The recent discovery of novel antiviral agents takes long time to be confirmed. So, the development of a strategy to treat pandemic diseases is of great importance and needed urgently. *Artemisia annua L.* has a long history of safety and great ability to treat hyperlipidemia, malaria and other recorded inflammatory diseases. Additionally, this plant has antimicrobial and antiviral activities [28].

The main health problem caused by SARS-CoV-2 is failure in the respiratory functions such as acute respiratory distress syndrome. The world is now seeking vaccines and alternative medicine that can alleviate the severe COVI-19 pandemic symptoms.

The main health problem caused by SARS-CoV-2 is represented by failure in the respiratory functions such as acute respiratory distress syndrome, world is now seeking for finding vaccines and alternative medicine that can alleviate the severe COVI-19 pandemic symptoms.

The finding of the current study greatly supported that our novel synthesized complex Art/Q/Zn has great ability as potent antiviral agent against pandemic virus "SARS-CoV-2" and also prohibited the antioxidant capacities , anti-hepatotoxicity and anti-pulmonary toxicity against toxicity induced by ACy in male rats and the obtained results are in great accordance with the previous results which demonstrated that clinical study indicated that treatment with one derivative of Artemisia markedly shorten the duration of the hospital stay for COVID-19 patients and decline their symptoms in China [62].

The key strength of this study included the in-depth analysis of the chemical characterisation of the novel complex (Art/Q/Zn) and confirmation of its chemical properties, behaviour and surface structure. This is the first study that has revealed that this novel complex (Art/Q/Zn) has high antiviral activities against SARS-Cov-2 with no-cytotoxicity effects. It has high antioxidant and antihepatotoxicity against oxidants and toxins induced by Acy, resulting from high temperatures of cooking food. This is a real challenge that threatens global health and, thus, this novel complex will benefit the general communities by its multi-characteristics, and it is potent antioxidant activity that will combat the current silent killer which is known as 'Oxidative damage'.

Deleted: characteristics

The findings extend our knowledge of the mechanism of action by which our novel complex (Art/Q/Zn) fights against the risky virus SARS-CoV-2. As for Artemisinin, SARS-CoV-2 is (+ve) single-stranded RNA virus; it has four essential proteins (spike, envelope, membrane and nucleocapsid). The SARS-CoV-2 invades host cells via two receptors: either angiotensin-converting enzyme 2 (ACE2) and/or CD147. The S-protein on SARS-CoV-2 virus binds to ACE2 or CD147 on the cellular host, mediating viral invasion to the host cells and its dissemination to other cells and, thus, inhibits viral entry, subsequent excessive viral replication, thereby mitigating SARS-CoV-2 disease [63].

It is known that two active components of Artemisia : Either Artemisinin or artesunate can retard the replication of the HCV, which is a positive sense virus and so similar to SARS-CoV-2 virus single-stranded RNA virus [60] Additionally, we confirmed in the current study the antiviral activity of our synthesized novel complex as it recorded high viral inhibition (IC50 equal 10.14 µg/ml) that can inhibit pandemic virus "SARS-CoV-2" viral invasion, replication and then reduce oxidative stress and thus eventually decline the inflammation during the pandemic of COVID-19 and these finding highlight the potential insights into the role of our novel synthesized complex in fighting against SARS-CoV-2 and elevate community health and immune system.

The current findings illustrate how the complex (Art/Q/Zn) inhibits the viral activity of SARS-CoV-2 through this proposed mechanism as shown in Fig (25). Both receptors ACE2 and CD147 in the host cells are main SARS-CoV-2 receptors [64-66]. The (S) spike protein

of SARS-CoV-2 can bind to the target cellular receptor either ACE2 or CD147 and enter the host cells, where the virus can replicate [67-68].

Thus, the main target mechanism is the ability of our synthesised novel complex Art/Q/Zn to decrease cellular receptor expression of ACE2, offering high protection against COVID-19 [68].

During viral entry into the cellular host, SARS-CoV-2 requires cellular proteases, such as trypsin-like proteases (TMPRSS2) that enhance the cleavage of the S protein to enhance fusion of the host cell membranes of the human and viral cellular membrane [69-70].

Previously, Art has been indicated to have high activity against malaria and other hepatic viruses induced in different hepatic diseases.

Art has an effective antiviral activity against different viruses such as HIV, Ebola and most corona viruses [71]. Recently, different medicinal plants such as Art have been tested against COVID-19 [72]. The current obtained results revealed ameliorative effect against lung congestion and this ameliorative effect may be attributed to the previous explanation of the mechanism of action of an Art derivative named Artesunate, which t inhibits invasion by cancer cells by expression of essential cellular proteases as previously demonstrated [73-75].

These findings confirmed the efficacy of the novel complex (Art/Q/Zn) in improving the pulmonary tissues due to the action of Art and synergistic effect of both Q and Zn in improving lung functions and may be due to the efficacy of Zn in eliminating viruses outside the cells thereby reducing the symptoms of SARS-CoV-2 on respiratory functions. Thus, this formula may be promising against any viral infections and severe oxidative stress.

Gendrot et al. [76] suggests that the mechanism of action of Art may involve inhibiting the binding of SARS-CoV-2 spike protein to (ACE2), the main binding cellular receptor, thereby preventing activation of SARS-CoV-2 and activation of natural killer cells [77].

Efferth., 2018 [78] confirms that Art may bind to E, N, $3CL^{Pro}$ and S protein. The main biological function of Art may be attributed to its ability to inhibit the functions of these viral proteins.

Deleted: N ,

The major health problem during the COVID-19 pandemic is the cytokine storm and elevated inflammatory markers, which induce oxidative stress which damages most of human organs [79]. Badraoui et al. [80] reported that Art extracts are safe for use, confirming the current results. These findings encourage usage of Art by oral route or by inhalation in order to capture the SARS-CoV-2 cells that make large colonies in the respiratory tract.

An additional strength of novel formula Art/Q/Zn is that Art binds to the target (6LU7) conferring stability to the formed complex, raising its inhibitory effect against SARS-CoV-2 for a long time.

Our obtained results are greatly reinforced by those of the previous study [80] that revealed that Artemisinin active compounds exhibited promising properties explaining the potent antioxidant, protective and healthy effects of ART.

Art as reported by [81] that Art interacted with different ways with ACE2, and this confirmed the potential antiviral effect of Art, and this action was enhanced after complexation with Q /Zn.

Deleted: ACE2

Deleted: Art

As previously reported that, Quercetin (Q) is considered as a naturally occurring flavonoid that shows multi-beneficial biological effects. Moreover, Q administration minimized the severe oxidative damage. Supplementation of Q plays an important role as protective agent by regulation of the inflammatory responses (especially those resulting from the viral infections) [35].

Beneficial effects of micronutrients in promotion of the immune response have earned more much attention. Particularly, micronutrients as Zn. Besides, Zn has a key role in the treatment of pulmonary diseases and subsequent dysfunction. In a previous analysis study, authors indicated that supplementation of Zn inhibited pneumonia. Meanwhile, low intake of dietary contains Zn, it could decline the human main resistance against infections greatly [81].

Therefore, our novel synthesized complex Art/Q/Zn decline the activity of these metalloenzymes and thus could be very essential for controlling the activity of severe infection of SARS-CoV-2.

Interestingly, previous studies reported that the expression proteases as TMPRSS2 protein and ACE2 can be up-regulated by androgens. So, we concluded that Art could induce degradation of androgen receptor through the 26S proteasome. Therefore, Art might inhibit the infection of SARS-CoV-2 by limiting expression of ACE-2 receptors or TMPRSS2 in host cells [28].

For CD147, it can elevate the synthesis of metalloproteinases in cell matrix and inflammatory cytokines. Art previously inhibited the expression of CD147 in human host cells. Additionally, Art strongly blocked CD147 expression. Therefore, Art might be highly effective in controlling of controlling and retarding the cytokine storm and thus inhibiting the infections by SARS-CoV-2 virus [28].

Addition of a great strength point to the high capacities of ART, is the proved great capacities of Q/Zn novel complex as our previous finding reporting the high antidiabetic and antioxidant activities of novel complex of Q/Zn and stem cell therapy [82] by complete chemical characterisation of this complex and our previous study reported that Q/Zn has a great benefits to the lung tissues and alleviate any inflammation due to diabetes mellitus induction as Olechnowicz et al. [83] reported that Zn can up-regulate the expression of inflammatory cytokines and also, Zinc as a metal plays a key role in the incidence of metabolic syndromes and may have a role in suppressing inflammation. Zn is required micronutrient to elevate the antioxidant enzymes that have the ability to scavenge free reactive radicals and thus declining the oxidative injury.

In complete agreement with the obtained results, Q/Zn has improved the antioxidant capacities of male rats as previously reported [35]as we revealed previously that Q/Zn interact with SOD and CAT enzymes and thus improve their antioxidant capacities in scavenging if free radicals and thus decreasing oxidative injury. Also, Q/Zn novel complex ameliorated pancreatic and pulmonary both histological and ultra-structures and this add more strength point to the current data that the novel synthesized mixed ligand of Aer/Q/Zn ameliorated greatly both hepatic and pulmonary structures and elevate antioxidant enzymes SOD, CAT and GSH with declining the final marker of lipid peroxidation MDA and thus alleviation of oxidative injury by great scavenging capacities to the free radicals induced by Acy administration.

The other bright side of the current study is the ability of the novel synthesized complex Art/Q/Zn in alleviation of oxidative stress, hepatotoxicity, pulmonary toxicity and both structural alterations induced by Acy as these results are consistent with data obtained in previous studies of [35] as they confirmed that Acy induced many pathological alterations and cellular injury occur due to the imbalance between antioxidant enzymes in tissues.

Hamza et al ,[31] demonstrated that ACR afforded significant elevation of MDA with decline in the antioxidant enzymes activities (SOD, CAT and GPx) and accordingly, Gedik et al. [84] who observed that Acy administration markedly declined the hepatic glutathione and thus it's administration induced severe hepatic injury and severe hepatocytes damage in structure and appeared clearly in TEM sections and histological sections with appearance of inflammatory cellular infiltration, necrosis and hemorrhage areas in hepatic tissues.

Additionally, Acy induced excessive production of free radicals with breakdown of the structure of polyunsaturated fatty acids in the cellular membranes and this leads to a deterioration of the complete cellular integrity and thus marked increment in both ALT and AST levels. In this study, elevated ALT, AST and LDH levels were observed in Acy liver cells due to the incidence of liver damage. This could be due to the introduction of enzymes such as ALT, AST and LDH into the blood circulation due to the destruction of the liver cellular membranes due to severe oxidative injury and elevated hepatic enzymes in the blood.

The obtained results and the high capacities of the novel synthesised complex Art/Q/Zn are in great accordance with a previous study [35], which reported that pulmonary fibrosis is greatly linked to enhanced oxidative stress and acute respiratory syndromes. Thus, pulmonary fibrosis is related greatly to the excessive progression of SARS-CoV-2, which leads to a high mortality rate during the COVID-19 pandemic. Hence, modulation of oxidative stress might be an essential concept for fighting against COVID-19 and its pulmonary fibrosis as Art/Q/Zn

Deleted: can

Deleted: ,

can attenuate the pulmonary fibrosis by up-regulating the antioxidant enzyme expression and elevating the antioxidant system against oxidative stress markers**.**

The findings of the current study broadly support the high capacities of the novel synthesised mixed ligand (Art/Q/Zn) as an antiviral and antioxidant agent with amelioration capacities in lowering high blood pressure and saving renal, hepatic and pulmonary functions.

5.Conclusion

The current findings have revealed the chemical structure of novel mixed ligand Art/Q/Zn and results of FT-IR showed that Zn (II) can be chelated via C=O and C–OH of the (Q) ligand and C=O of the Art ligand forming (Art/Q/Zn) complex with chemical formula $[Zn(Q)(Art)(Cl)(H_2O)_2].3H_2O$. The novel complex has a high anti-SARS-CoV-2 activity at a low concentration (IC_{50} = 10.14 µg/ml) and without any cytotoxicity to the cellular host (CC_{50}= 208.5 µg/ml). It alleviated the toxicity of Acy hepatic and pulmonary toxicity by improving all biochemical markers and was effective in lowering systolic or diastolic blood pressure and regulating heart beats after Acy administration. The Art/Q/Zn complex has antioxidant capacities against oxidative stress and has high antiviral activity against (SARS-CoV-2). It also has high abilities to ameliorate organ physiological functions and regulation of ACE-2 receptors and thus reduce inflammation markers during the COVID-19 pandemic.

Acknowledgment: The researchers would like to acknowledge Deanship of Scientific Research, Taif University for funding this work.

Conflict of Interest: Authors declare no conflict of interest

References

1. **Mohapatra RK, Mahal A, Kutikuppala LVS, Pal M, Kandi V, Sarangi AK, Obaidullah AJ and Mishra S. 2022.** Renewed global threat by the novel SARS-CoV-2 variants 'XBB, BF.7, BQ.1, BA.2.75, BA.4.6': *A discussion. Front. Virol.* **2** 1077155.
2. **Mohapatra RK, Kandi V, Verma S, Dhama K. 2022.** Challenges of the omicron (B.1.1.529) variant and its lineages: A global perspective. *Chem BioChem*. **23** e202200059.
3. **Mohapatra RK, Kandi V, Sarangi AK, Verma S, Tuli HS, Chakraborty S, et al. 2022.** The recently emerged BA.4 and BA.5 lineages of omicron and their global health concerns amid the ongoing wave of COVID-19 pandemic. *Int J Surg*. **103** 106698.
4. **Dhawan M, Priyanka, Choudhary OP. 2022.** Omicron SARS-CoV-2 variant: Reasons of emergence and lessons learnt. *Int J Surg*. 97 106198.
5. **Mohammad A, Prakash KS, Ranjan KM, Manjeet K, Azaj A, Soo M, Arunabhiram C, Saud JA, Susanta KB. 2022.** Structural investigations, Hirsfeld surface analyses, and molecular docking studies of a phenoxo-bridged binuclear Zinc(II) complex. *Journal of Molecular Structure* **1251** 132039.
6. **Mohammad A, Saikh MW, Mahboob A, Agata TK, Rafal K, Saud IA, Resayes, Fahad FA, Mohammad RK, Rajendra. 2021.** Design, structural investigations and antimicrobial activity of pyrazole nucleating copper and zinc complexes. *Polyhedron*. **195** 114991.
7. **Rajan R, Deeksha S, PremPrakash S, Bhanu S, Vikas K, Brijesh R, Mansi V, Anuradha S, David J, Kamal D. 2021.** Phytocompounds of *Rheum emodi*, *Thymus*

Deleted: Research ,

Deleted: S .

Deleted: *Surg*, 97

Deleted: A ,

Deleted: K, Azaj

Deleted: A, Soo

Deleted: M, Arunabhiram

Deleted: IA, Susanta

Deleted: Resayes, Fahad

Formatted: Font: Italic

Formatted: Font: Italic

serpyllum, and *Artemisia annua* Inhibit Spike Protein of SARS-CoV-2 Binding to ACE2 Receptor: In Silico Approach. *Current Pharmacology Reports.* **1** 15.7

8. **Xinyu L, Huijun Y, Xiaozhen L, Hongliang W. 2023.** Spike protein mediated membrane fusion during SARS-CoV-2 infection. *Journal of medical virology* **95(1)** e28212.
9. **Al-Shemary RK, Ranjan KM, Manjeet K, Ashish K, Mohammad A, Hardeep ST, Azaj A, Pranab K, Mohapatra g, Kuldeep D. 2023.** Synthesis, structural investigations, XRD, DFT, anticancer and molecular docking study of a series of thiazole-based Schiff base metal complexes. *Journal of Molecular Structure* **1275** 134676.
10. NIH, COVID-19 treatment guidelines, www.covid19treatmentguidelines.nih.gov, Last updated on April 20,2023. Accessed on?
11. **Mohapatra RK, Mohammad A, PranabK. MA, Mohnad A, Lina P, Oval Y, Saud IA, Kim JD, Kuldeep D, Azaj A, Veronique S, Sarika V, Mukesh KR. 2022.** Computational studies on potential new anti-Covid-19 agents with a multi-target mode of action. *Journal of King Saud University -Science*. **34** 102086.
12. **Ranjan KM, Satwik K, Tarun KS, Venkataramana K, Ajit B, Sarika V, Kudrat-E, Susanta KB, Taghreed HA, Marei ME, Ashish K. Sarangi, Kuldeep Dhama.2022.** SARS-CoV-2 and its variants of concern including Omicron: A never ending pandemic. *Chemical Biology and Drug Design* **99(5)** 769-788.
13. **Babcock GJ, Esshaki DJ, Thomas WD, Ambrosino DM. 2004.** Amino acids 270 to 510 of the severe acute respiratory syndrome coronavirus spike protein are required for interaction with receptor. *J Virol.* **78** 4552–60.
14. **Wong SK, Li W, Moore MJ, Choe H, Farzan MA. 2004.** 193-amino acid fragment of the SARS coronavirus S protein efficiently binds angiotensin-converting enzyme 2. *Int J Biol Chem Sci.* **279** 3197–201.
15. **Anand K, Ziebuhr J, Wadhwani P, Mesters JR, Hilgenfeld. 2003.** Coronavirus main proteinase (3CLpro) structure: basis for design of anti-SARS drugs. *Science* **300** 1763–7.
16. **Perlman S, Netland J. 2009.** Coronaviruses post-SARS: update on replication and pathogenesis. *Nat Rev Microbiol.* **7** 439–50.
17. **Dimitrov DS. 2003.** The secret life of ACE2 as a receptor for the SARS virus. *Cell* 115 652–3.
18. **Mohnad A, Mohapatra KR, Ashish KS, Pranab KM, Eltayb WA, Mahboob A, Amr AE, Mohammad A, Saud IA, Veronique S, Kuldeep D. 2021.** In silico studies on phytochemicals to combat the emerging COVID-19 infection. *Journal of Saudi Chemical Society*. **25(12)** 101367.
19. **Joshi T, Joshi T, Sharma P, Mathpal S, Pundir H, Bhatt V, Chandra S.2020.** In silico screening of natural compounds against COVID-19 by targeting Mpro and ACE2 using molecular docking. *European Review for Medical and Pharmacological Sciences.* **24(8)** 4529-4536.
20. **Şevki A, Volkan E, Iqra S, Azhar R, Ameer FZ, Muhammad A, Mohnad A, Ibrahim MI, Abdo AE. 2021.** Caffeic acid derivatives (CAFDs) as inhibitors of SARS-CoV-2: CAFDs-based functional foods as a potential alternative approach to combat COVID-19. *Phytomedicine.* **85** 153310.
21. **Hamza RZ, Gobouri AA, Al-Yasi HM, Tarek AA, Samy ME. 2021.** A New Sterilization Strategy Using TiO_2 Nanotubes for Production of Free Radicals that Eliminate Viruses and Application of a Treatment Strategy to Combat Infections Caused by Emerging SARS-CoV-2 during the COVID-19 Pandemic. *Coatings* **11(6)** 680.
22. **Xiao X, Chakraborti S, Dimitrov AS, Gramatikoff K, Dimitrov DS.2003.** The SARS-CoV S glycoprotein: expression and functional characterization. *Biochem Bioph Res Co.* **312** 1159–64.
23. **Iyengar MA. 1985.** Study of crude drugs. 2nd ed. Manipal: *College of Pharmaceutical Sciences* 13–78.

Formatted: Font: Italic
Deleted: KM ,
Deleted: A ,
Deleted: thiazole based
Deleted: NIH,COVID
Formatted: Highlight
Deleted: *Cell* 115
Deleted: A, Mohapatra
Deleted: KR, Ashish
Deleted: KS, Pranab
Deleted: KM, Eltayb
Deleted: WA, Mahboob
Deleted: A, Amr
Deleted: AE, Mohammad
Deleted: FZ, Muhammad
Deleted: A , Mohnad
Deleted: A, Ibrahim
Deleted: MI, Abdo

24. **Ye X, Jianrong H. 2021.** Anti-malarial drug: the emerging role of artemisinin and its derivatives in liver disease treatment. *Chinese Medicine*.**16** 80.
25. **Hardy T**, **Mann DA. 2016.** Epigenetics in liver disease: from biology to therapeutics. *Gut.* **65(11)** 1895–905.
26. **Pimpin L, Cortez-pinto H, Negro F, Corbould E, Lazarus J, Webber L, Sheron N.2018.** EASL HEPAHEALTH Steering Committee. Burden of liver disease in Europe: Epidemiology and analysis of risk factors to identify prevention policies. *J Hepatol.* **69(3)** 718–35.
27. **Wang FS, Fan J, Zhang Z, Gao B and Wang H. 2014.**The global burden of liver disease: the major impact of China. *Hepatology.* **60(6)** 2099–108.
28. **Grant DM.1991.**Detoxifcation pathways in the liver. *J Inherit Metab Dis*. **14(4)** 421–30.
29. **Sarin SK, Kumar M, Eslam M, George J, Al-Mahtab M, Akbar SMF, Jia J, Tian Q, Aggarwal R, Muljono D, Omata M, Ooka Y, Han K, Lee H, Jafri W, Butt A, Chong C, Lim S, Pwu R, Chen D. 2020.** Liver diseases in the Asia-Pacific region: a Lancet Gastroenterology & Hepatology Commission. *Lancet Gastroenterol Hepatol.* **5(2)** 167–228.
30. **Iftekhar A, Rahman A, Monyck JSL, Carl HDS and Faiz UlH. 2022.** *Artemisia annua L.* and Its Derivatives: Their Antiviral Effects on COVID-19 and Possible Mechanisms. *Journal of Exploratory Research in Pharmacology* **7(1)** 54-58.
31. **Hamza RZ, AL-thubaiti EH, Omar AS. 2019.** The Antioxidant Activity of Quercetin and its Effect on Acrylamide Hepatotoxicity in Liver of Rats. *Lat. Am. J. Pharm.* **38(10)** 2057-62.
32. **Kerim Y, Recep E, Aydin G, Tuba D, Emine S.2022.** Evaluation of the protective effects of morin against acrylamide-induced lung toxicity by biomarkers of oxidative stress, inflammation, apoptosis, and autophagy. *Journal of food biochemistry* e14111.
33. **Zeynep E, Erman E, Harika GB, Eyup A. 2022.** Effects of Acrylamide and Crocin on rat lung tissue. *Annals of Medical Research* 29**(4)** 397-400.
34. **Erdemli Z, Erdemli ME, Turkoz Y, Gul M, Yigitcan B, Bag HG. 2019.** The effects of acrylamide and Vitamin E administration during pregnancy on adult rats' testis. *Andrologia.* **51** e13292.
35. **Hamza RZ, Al-Motaani SE and Malik N. 2019.** Protective and Antioxidant Role of Selenium Nanoparticles and Vitamin C Against Acrylamide Induced Hepatotoxicity in Male Mice. *Int. J. Pharmacol.* **15** 664-674.
36. **Zarezade V, Moludi J, Mostafazadeh M, Mohammadi M, Veisi A. 2018.** Antioxidant and hepatoprotective effects of Artemisia dracunculus against CCl4-induced hepatotoxicity in rats. *Avicenna J Phytomed*, **8(1) 51**-62.
37. **Refat MS, Hamza RZ, Adam AMA, Saad HA, Gobouri AA, Al-Harbi FS, Al-Salmi FA, Altalhi T, El-Megharbel SM.** Quercetin/Zinc complex and stem cells: A new drug therapy to ameliorate glycometabolic control and pulmonary dysfunction in diabetes mellitus: Structural characterization and genetic studies. *PLoS ONE* **16(3)** e0246265.
38. **Vessal M, Hemmati M, Vasei M. 2003.** Antidiabetic effects of quercetin in streptozotocin-induced diabetic rats. *Comp. Biochem. Physiol. C Toxicol. Pharmacol.* **135C** 357–364.
39. **Maret W. 2017.** Zinc in Pancreatic Islet Biology, Insulin Sensitivity, and Diabetes. Prev. *Nutr. Food Sci*. **22** 1–8.
40. **Lassi ZS, Moin A, Bhutta ZA. 2016.** Zinc supplementation for the prevention of pneumonia in children aged 2 months to 59 months. *Cochrane Database of Systematic Reviews* 12 7350.

Deleted: X, Jianrong

Deleted: EH ,

Deleted: *Research* **29**

Deleted:) 397

Deleted: rats

Deleted: **15** 664

Deleted:) 51

Deleted: *Reviews* **12**

41. **O'Neil MJ. (ed.).2006.** The Merck Index-An Encyclopedia of chemicals, Drugs, and Biologicals. Whitehouse Station, NJ: Merck and Co., Inc., P.1211.
42. **El-Megharbel SM, Alsawat M, Al-Salmi FA, Hamza RZ. 2021.** Utilizing of (Zinc Oxide Nano-Spray) for Disinfection against "SARS-CoV-2" and Testing Its Biological Effectiveness on Some Biochemical Parameters during (COVID-19 Pandemic)—" ZnO Nanoparticles Have Antiviral Activity against (SARS-CoV-2)". Coatings 11 388.
43. **Ohkawa H, Ohishi N, Yagi K. 1979.** Assay for lipid peroxides in animal tissues by thiobarbituric acid reaction. *Analytical biochemistry.* **95(2)** 351-358.
44. **Sun Y, Oberley LW, Li YA. 1988.** Simple method for clinical assay of superoxide dismutase. *Clinical Chemistry.* **34** 497-500.
45. **Aebi, 1984.** Catalase in vitro. *Methods in Enzymology*.**105** 121-126.
46. **Paglia DE, Valentive WN. 1967.** Studies on the quantitative and qualitative characterization of erythrocyte glutathione peroxidase. *Journal of Laboratory Clinical Medicine* ***70*** 158-69.
47. **Abubakar MG, Ukwuani AN, Mande UU. 2015.** Antihypertensive activity of Hibiscus Sabdariffa aqueous calyx extract in Albino rats. *Sky Journal of Biochemistry Research* **4 (3)** 16-20.
48. **Swiss Target Prediction: updated data and new features for efficient prediction of protein targets of small molecules, Nucl. Acids Res. (2019).** For technical information about the prediction algorithm, Shaping the interaction landscape of bioactive molecules, Bioinformatics. 29 (2013) 3073-3079.
49. **Abo Elmaaty A, Eldehna WM, Khattab M, Kutkat O, Alnajjar R, El-Taweel AN, Al-Rashood ST, Abourehab MAS, Binjubair FA, Saleh MA. 2022.** Anticoagulants as Potential SARS-CoV-2 Mpro Inhibitors for COVID-19 Patients: In Vitro, Molecular Docking, Molecular Dynamics, DFT, and SAR Studies. *Int. J. Mol. Sci.* **23** 12235.
50. **Dean A, Sullivan K, Soe M. 2013.** OpenEpi: Open-Source Epidemiologic Statistics for Public Health. Updated 2013/4/6. https://www.OpenEpi.com. Accessed on?? Is this the exact link?
51. **El-Megharbel SM, Hamza RZ. 2022.** Synthesis, spectroscopic characterizations, conductometric titration and investigation of potent antioxidant activities of gallic acid complexes with Ca (II), Cu (II), Zn(III), Cr(III) and Se (IV) metal ions. *Journal of Molecular Liquids* **358** 119196.
52. **Nakamoto K. 1986.** Infrared and Raman Spectra of Inorganic and Coordination Compounds, fourth ed., Wiley, New York.
53. **Nakamoto K. 1970.** Infrared Spectra of Inorganic and Coordination Compounds, Wiley Interscience, John Wiley & Sons, New York, NY, USA, 2nd edition.
54. **Bellamy LJ. 1975.** The Infrared Spectra of Complex Molecules, Chapman and Hall, London, UK.
55. **Sanna D, Ugone V, Fadda A, Micera G, Garribba E. 2016.** Behavior of the potential antitumor V(IV)O complexes formed by flavonoid ligands. 3. Antioxidant properties and radical production capability. *J. Inorg. Biochem*. **161** 18–26.
56. **Charisiadis P, Kontogianni VG, Tsiafoulis CG, Tzakos AG, Siskos M, Gerothanassis IP. 2014.** ^{1}H-NMR as a Structural and Analytical Tool of Intra- and Intermolecular Hydrogen Bonds of Phenol-Containing Natural Products and Model Compounds. *Molecules.* **19** 13643-13682.

Deleted: MJ.(
Deleted: chemicals ,
Deleted: Drugs ,
Deleted: Station ,NJ
Deleted: —"ZnO
Deleted: Coatings 11
Deleted: Ohkawa H
Deleted: avantitaue
Deleted: gualitative
Deleted: *Research* 4
Deleted: Open Source
Formatted: Highlight
Deleted: Charisiadis P
Deleted: Kontogianni VG
Deleted: Tsiafoulis CG
Deleted: Tzakos AG
Deleted: Siskos M

57. **Hamza RZ, Alaryani FS, Alotaibi RE, Al-Harthi MA, Alotaibi GS, Al-Subaie NA, Al-Talhi AA, Al-Bogami B, Al-Baqami NM, El-Megharbel SM, Al-Thubaiti EH. 2022.** Efficacy of Prednisolone/Zn Metal Complex and Artemisinin Either Alone or in Combination on Lung Functions after Excessive Exposure to Electronic Cigarettes Aerosol with Assessment of Antibacterial Activity. *Crystals* **12** 972.
58. **Al-Thubaiti EH, El-Megharbel SM, Albogami B, Hamza RZ. 2022.** Synthesis, Spectroscopic, Chemical Characterizations, Anticancer Capacities against HepG-2, Antibacterial and Antioxidant Activities of Cefotaxime Metal Complexes with Ca (II), Cr (III), Zn (II), Cu (II) and Se (IV). Antibiotics **11** 967.
59. **Lever ABP.** 1984. Inorganic Electronic Spectroscopy, 2nd ed., Elsevier, Amsterdam.
60. **Hamza RZ, Gobouri AA, Al-Yasi HM, Al-Talhi TA, El-Megharbel SM. 2021.** New Sterilization Strategy Using TiO_2 Nanotubes for Production of Free Radicals that Eliminate Viruses and Application of a Treatment Strategy to Combat Infections Caused by Emerging SARS-CoV-2 during the COVID-19 Pandemic. *Coatings* 11 680.
61. **Khan MAAA, Jain DC, Bhakuni RS, Zaim M, Thakur RS.1991.** Occurrence of some antiviral sterols in Artemisia annua. *Plant Sci* 75**(2)** 161– 165.
62. **Karamoddini M, Emami S, Ghannad M, Sani E, Sahebkar A. 2017.** Antiviral activities of aerial subsets of Artemisia species against Herpes Simplex virus type 1 (HSV1) in vitro. *Asian Biomedicine* **5(1)** 63–68.
63. **Uzun T, Toptas O. 2020.** Artesunate: could be an alternative drug to chloroquine in COVID-19 treatment? *Chin Med* **15** 54.
64. **Kapepula PM, Kabengele JK, Kingombe M, Van Bambeke F, Tulkens PM, Sadiki Kishabongo A, Decloedt E, Zumla A, Tiberi S, Suleman F, Tshilolo L, TamFum JJM, Zumla A, Nachega J. 2020.** *Artemisia spp.* derivatives for COVID-19 treatment: Anecdotal use, political hype, treatment potential, challenges, and road map to randomized clinical trials. *Am J Trop Med Hyg* **103(3)** 960–964.
65. **Ulrich H, Pillat MM. 2020.** CD147 as a Target for COVID-19 Treatment: Suggested Effects of Azithromycin and Stem Cell Engagement. *Stem Cell Rev Rep.* **20** 1–7.
66. **Shereen MA, Khan S, Kazmi A, Bashir N, Siddique R. 2020.** COVID-19 infection: Origin, transmission, and characteristics of human coronaviruses. *J Adv Res* **24** 91–98.
67. **Ulrich H, Pillat MM**. 2020. CD147 as a target for COVID-19 treatment: suggested effects of azithromycin and stem cell engagement. *Stem Cell Rev Rep* **16(3)** 434–440.
68. **Kaptein SJ, Efferth T, Leis M, Rechter S, Auerochs S, Kalmer M, Bruggeman C, Vink C, Stamminger T, Marschall M. 2006.** The anti-malaria drug artesunate inhibits replication of cytomegalovirus in vitro and in vivo. *Antiviral Res* **69(2)** 60–69.
69. **Wang K, Chen W, Zhou YS, Lian JQ, Zhang Z, Du P, Li G, Yang Z, Hong-YC, Jie-Jie G, Bin W, Xiu-Xuan S, Chun-Fu W, Xu Y, Peng L, Yong QD, Ding W, Xiang-Min Y, Yu-Meng Z, Kui Z, Zhao-Hui Z, Jin Lin M, Ting G, Ying S, Jun Z, Ling F, Qing-Yi W, Huijie Bian, Ping Zhu, Zhi-Nan C. 2020.** SARS-CoV-2 invades host cells via a novel route: CD147-spike protein. *BioRxiv* [Preprint] 2020:2020.03.14.988345. Now published in *Signal Transduction and Targeted Therapy* doi: 10.1038/s41392-020-00426-x
70. **Elkhodary MSM. 2020.** Treatment of COVID-19 by controlling the activity of the nuclear factor-Kappa B. *Cell Bio* **9(2)** 109–121.

Deleted: -
Deleted:
Deleted: 1984
Deleted: *Coatings* **11**
Deleted: *Sci* **75**
Deleted: Bruggeman C
Formatted: Highlight
Formatted: Highlight

71. **Augustin Y, Staines H, Kamarulzaman A, Platteeuw H, Krishna S. 2020.** Artesunate may attenuate the effects of Cytokine Release Syndrome (CRS) in Covid-19 disease by targeting Interleukin-6 and associated inflammatory response pathways. OSF Preprints 2020.

72. **Hoffmann M, Kleine-Weber H, Schroeder S, Krüger N, Herrler T, Erichsen S, Schiergens TS, Georg H, Nai-Huei W, Andreas N, Marcel AM, Christian D, Stefan P. 2020.** SARS-CoV-2 cell entry depends on ACE2 and TMPRSS2 and is blocked by a clinically proven protease inhibitor. *Cell* **181(2)** 271–280.e8.

73. **D'alessandro S, Scaccabarozzi D, Signorini I, Perego F, Ilboudo, DP, Ferrante P. 2020.** The use of antimalarial drugs against viral infection. *Microorganisms* **8** 1-26.

74. **Kalalagh KF, Kashkooli AB, Babaei A, Rezaei A, der Krol AR.2022.** Artemisinins in combating viral infections like SARS-CoV-2, Inflammation and cancers and options to meet increased global demand.*Front.Plant.Sci.***13** 780257.

75. **Rasheed SAK, Efferth T, Asangani IA, Allgayer H. 2010.** First evidence that antimalarial drug artesunate inhibits invasion and *in vivo* metastasis in lung cancer by targeting essential extracellular proteases. *Int. J. cancer.* **127(6)** 1475-1485.

76. **Gendrot M, Duflot I, Boxberger M, Delandre O, Jardot, P, Le Bideau M. 2020.** Antimalarial artemisinin-based combination therapies (ACT) and COVID-19 in Africa: in vitro inhibition of SARS-CoV-2 replication by mefloquine-artesunate. *Int. J. Infect. Dis.* **99** 437-440.

77. **Rolta R, Salaria D, Kumar V, Sourirajan A, and Dev K. 2020.** Phytocompounds of *Rheum emodi, Thymus serpyllum* and *Artemisia annua* inhibit COVID-19 binding to ACE2 receptor in silico approach. *Current Pharmacology Reports* **7(1)** 1-15.

78. **Efferh T. 2018.** Beyond malaria: the inhibition of viruses by artemisinin –type compounds. *Biotechnol.Adv.***36** 1730-1737.

79. **Krishna S, Ganapathi S, Ster IC, Saeed MEM, Cowan M, Finlayson CA. 2015.** randomized, double blind, placebo-controlled pilot study of oral artesunate therapy for colorectal cancer. *EbioMedicine* **2** 82-90.

80. **Badraoui R, Saoudi M, Hamadou W, Elkahoui S, Siddiqui AJ, Alam JM, Jamal A, Adnan M, Suliemen AME, Alreshidi MM, Yadav DK, Naili H. and Ben-Nasr, H. 2022.** Antiviral effects of Artemisinin and it's derivatives against SARS-CoV-2 Main proteases: Computational Evidences and interactions with ACE2 Allelic variants. *Pharmaceuticals.*15-129.

81. **Ben Nasr H, Badraoui R. 2022.** Approach of utilizing Artemisia herbs to treat COVID-19. *Braz.J. Pharm. Sci.* **58:** e20345.

82. **Maret W. 2017.** Zinc in Pancreatic Islet Biology, Insulin Sensitivity, and Diabetes. Prev. Nutr. *Food Sci.* **22** 1–8.

83. **Olechnowicz J, Tinkov A, Skalny A, Joanna S. 2018.** Zinc status is associated with inflammation, oxidative stress, lipid, and glucose metabolism. *J Physiol Sci.* **68** 19 - 31.

84. **Gedik S, Erdemli ME, Gul M, Yigitcan B, Bag HG, Aksungur Z, Altinoz E. 2017.** Hepatoprotective effects of crocin on biochemical and histopathological alterations following acrylamide-induced liver injury in Wistar rats. *Biomed. Pharmacother* **95** 764-770.

Deleted: S, Schiergens
Deleted: D ,
Deleted: A ,
Deleted: 2 ,
Deleted: Rasheed SAK
Deleted: Asangani IA
Formatted: Font: Italic
Deleted: M ,
Deleted: Africa :
Deleted: Dev K.
Deleted: approach .
Deleted: randomized ,
Deleted: Suliemen AME
Deleted: i
Deleted: .
Deleted: Z, Altinoz

Table 1: Tools and synthesis analysis.

Analysis instrument	Models
Elemental analysis	PerkinElmer CHN(S (?) 2400 Elemental Analyzer
Conductance	Jenway 4010 conductivity meter
FTIR spectra	Bruker FT-IR Spectrophotometer
Electronic spectra	ATi Unicam UV2 UV/VIS Spectrometer ?
TEM	JEOL 100s transmission electron microscope (TEM) – confirm
Magnetic measurements	Sherwood Scientific Magnetic Balance using Gouy method
SEM	Quanta 250 FEG (ESEM) Scanning Electron Microscope
X-ray diffraction patterns	X 'Pert PRO PANanalytical X-ray powder diffraction, target copper with secondary monochromate.

I can't align the cells in orange shadding to the left. Please, format the table so that everything looks consistent!

Formatted: Left

Formatted: Font: Bold

Formatted: Justified

Formatted Table

Deleted:

Formatted: Font colour: Red

Formatted: Highlight

Formatted: Space Before: 0 pt

Formatted

Formatted

Deleted: UV2 Unicam (UV/Vis Spectrophotometer)

Formatted: Highlight

Formatted

Deleted: microscopy

Formatted: Highlight

Formatted: Font colour: Red

Formatted: Space Before: 0 pt

s **:Deleted**

m **:Deleted**

b **:Deleted**

Formatted: Justified, Space Before: 0 pt, After: 0 pt

Deleted: 250

Deleted: equipment

Formatted: Justified, Space Before: 0 pt, After: 0 pt

Formatted: Space Before: 0 pt

Formatted: Space Before: 0 pt

Formatted: Space Before: 0 pt, After: 0 pt, Tab stops: 3,81 cm, Left + 4,13 cm, Left

Formatted: Justified

Table 2. Electronic spectra and magnetic moments of quercetin, artemisinin and their zinc mixed ligand.

Sample	Electronic bands/ nm		Magnetic moment	Geometry
	π–π*	n–π*		
Quercetin	294	365	-	-
Artemisinin	295	354	-	-
$Zn(Q)(Art)(Cl)(H_2O)_2].3H_2O$	290	345	diamagnetic	Octahedral

Deleted: their zinc

Formatted: Font: Bold

Formatted Table

Table 3. Assessment of Art/Q/Zn (30 mg/Kg) on hepatic function and enzyme activity of male rats treated with Acy (500 mg/Kg) for successive 30 days.

Parameters	Control	Acy (500 mg/Kg)	Art/Q/Zn (30 mg/Kg)	Acy +Art/Q/Zn
ALT (U/L)	13.14±1.09^{b}	184.91±8.42^{c}	13.25±1.24^{b}	26.44±2.72^{bc}
AST (U/L)	14.15±1.26^{b}	294.52±9.73^{b}	14.05±1.82^{b}	24.10±2.63^{c}
LDH (U/L)	140.74±8.19^{a}	545.40±12.76^{a}	142.13±8.51^{a}	198.86±9.71^{a}

Values are expressed as mean ± SE and, n=10. ALT, alanine aminotransferase; AST, aspartate aminotransferase; and LDH, lactate dehydrogenase.

a, b, c meaning??

Deleted: s

Formatted Table

Deleted: (

Deleted:)

Formatted: Font colour: Red, Highlight

Formatted: Font colour: Red

Formatted: Default Paragraph Font, Font: Palatino Linotype, 10 pt, Font colour: Red

Formatted: MDPI_3.1_text, Left, Right: 0 cm

Formatted: Font: Palatino Linotype, 10 pt

Table 4. The effects of Art/Q/Zn (30 mg/Kg) on inflammatory markers within male rats exposed to either Acy (500 mg/Kg) alone or in combination with Art/Q/Zn for 30 successive days.

Groups	IL-6 (Pg/g)	TNF-α (Pg/g)	CRP (mg/L)
Control	3.40±0.53^{c}	4.48±0.10^{cd}	2.24±0.21^{d}
Acy (500 mg/Kg)	49.70±4.62^{a}	62.75±4.54^{a}	96.10±3.79^{a}
Art/Q/Zn(30 mg/Kg)	3.82±0.73^{c}	3.80±0.88^{d}	4.24±0.97^{c}
Acy + Art/Q/Zn	6.43±1.23^{b}	10.75±1.39^{b}	6.51±0.91^{b}

Values were expressed as mean ± SE; n = 10. IL-6; interleukin-6, TNF-α; Tumor necrosis factor Alpha and CRP; C-Reactive protein.

Letters are assigned alphabetically to indicate significance ($P < 0.05$) as compared to the control group and other treated groups. -> this is not clear enough! Be specific

Deleted: levels
Deleted: in
Deleted: treated with
Deleted: successive
Deleted: or their combinations for 30 successive days
Formatted: Space Before: 3 pt, After: 3 pt
Formatted Table
Formatted: Font: Not Bold
Formatted: Space Before: 3 pt, After: 3 pt
Formatted: Font: Not Bold
Formatted: Font: Not Bold
Formatted: Font: Not Bold
Formatted: Space Before: 3 pt, After: 3 pt
Formatted: Font: Not Bold
Formatted: Space Before: 3 pt, After: 3 pt
Formatted: Space Before: 3 pt, After: 3 pt
Formatted: Font: Not Bold
Formatted: Space Before: 3 pt, After: 3 pt
Deleted: (
Deleted:)
Deleted: Alpha and
Formatted: Highlight

Table 5. The effect of Art/Q/Zn (30 mg/Kg) on the antioxidant status of rats or mice?? liver tissues after treatment with Acy alone, Art/Q/Zn alone, or their combined administration for 30 successive days.

Groups	MDA (nmoles of MDA /g)	CAT (nmol/g of protein/min)	SOD (U/g of protein)	GPx (nmol/g of protein/min)
Control	4.13±1.92^{c}	11.79±1.47^{a}	16.59±1.62^{b}	12.73±1.49^{a}
Acy (500 mg/Kg)	53.42±5.79^{a}	2.49±0.86^{c}	5.47±1.44^{d}	5.32±1.48^{d}
Art/Q/Zn (30 mg/Kg)	4.40±1.25^{c}	12.57±1.81^{a}	17.76±1.65^{ab}	12.95±2.69^{a}
Acy+ Art/Q/Zn	14.13±1.16^{b}	4.21±0.95^{b}	13.89±1.58^{c}	10.45±1.98^{b}

Values are expressed as mean ± SE; n=10. MDA; malondialdehyde, CAT; catalase, SOD; superoxide dismutase, GPx; glutathione peroxidase.

Symbols ?? are different alphabetically to indicate significance ($P < 0.05$) as compared to the control group and other treated groups -> same as previously!

Formatted: Highlight

Deleted: and/

Deleted: combinations

Deleted: (

Deleted:)

Deleted: catalase, SOD

Formatted: Font colour: Red, Highlight

Table 6. Assessment of Art/Q/Zn (30 mg/Kg) on blood pressure (Systolic, Diastolic and heart rate) levels of male rats treated with Acy (500 mg/Kg) for successive 30 days.

Just Acy, or also the complex, and the combination of Acy and the complex! Be consisten and clear in the legends too!

Groups	Systolic (mmHg)	Diastolic (mmHG)	Heart rate (Pulse/min)
Control	134.90±4.02^{b}	108.74±2.58^{b}	263.21±5.69^{c}
Acy	188.20±3.64^{a}	162.02±5.25^{a}	297.08±4.68^{b}
Art/Q/Zn	102.05±1.36^{c}	82.94±5.69^{c}	379.78±5.68^{a}
Acy + Art/Q/Zn	134.95±5.02^{b}	108.75±6.25^{b}	263.54±3.68^{c}

??What are the letterS??? further notes

Deleted: Systolic ,

Deleted:

Deleted:

Formatted: Highlight

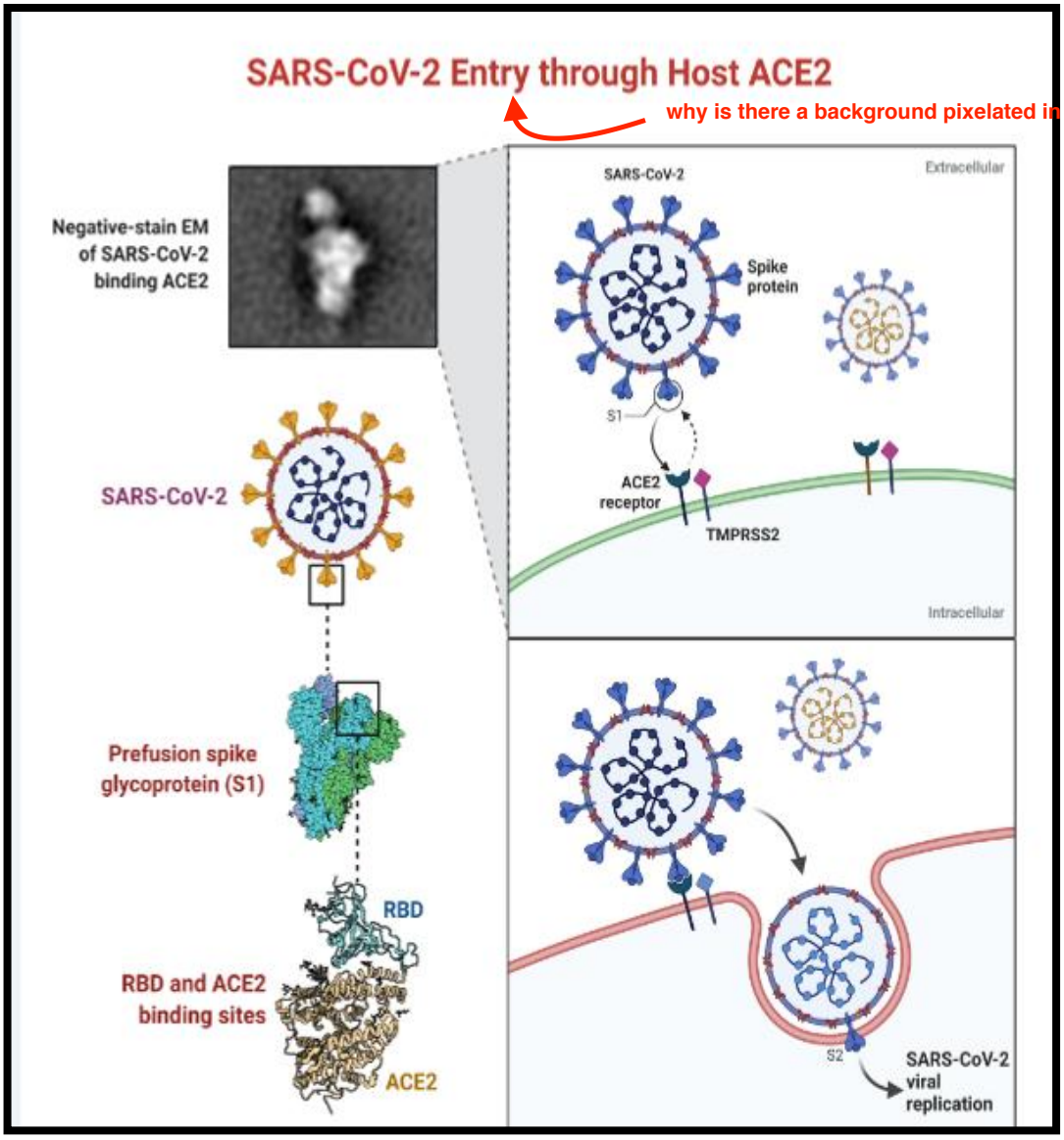
SARS-CoV-2 Entry through Host ACE2
why is there a background pixelated in here?
Negative-stain EM of SARS-CoV-2 binding ACE2
SARS-CoV-2
Prefusion spike glycoprotein (S1)
RBD
RBD and ACE2 binding sites
ACE2
SARS-CoV-2
Extracellular
Spike protein
S1
ACE2 receptor
TMPRSS2
Intracellular
S2
SARS-CoV-2 viral replication

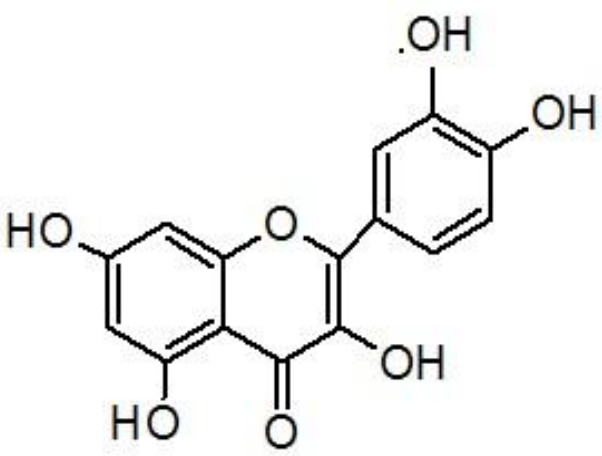

(A)

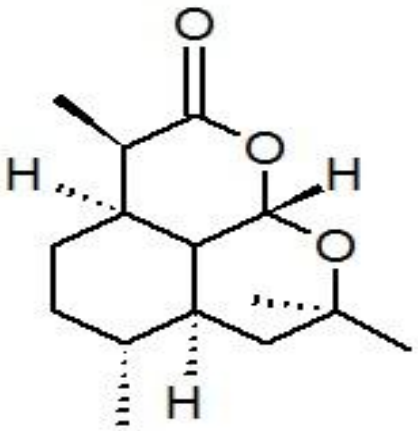

(B)

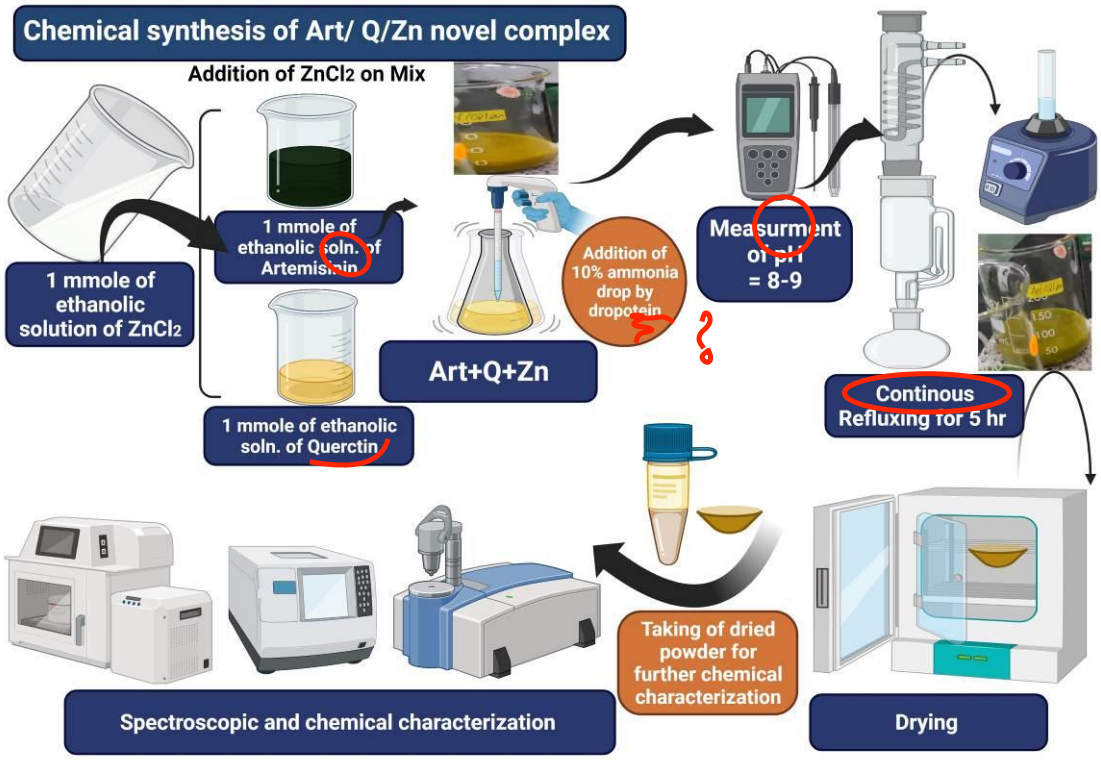
Chemical synthesis of Art/ Q/Zn novel complex
Addition of ZnCl2 on Mix
1 mmole of ethanolic solution of ZnCl2
1 mmole of ethanolic soln. of Artemisinin
1 mmole of ethanolic soln. of Quercetin
Art+Q+Zn
Addition of 10% ammonia drop by dropwise
Measurment of pH = 8-9
Continous Refluxing for 5 hr
Drying
Taking of dried powder for further chemical characterization
Spectroscopic and chemical characterization

Timeline experimental design

Experimental timeline for (Acy) and novel complex (Art/Q/Zn)

treatments?

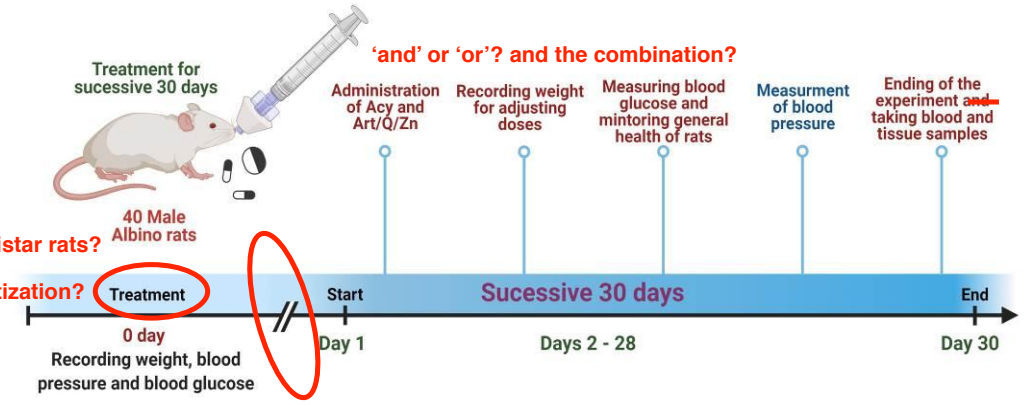

'and' or 'or'? and the combination?

Wistar rats?

treatment of acclimatization?

there is no break in the timeline, why is this here?

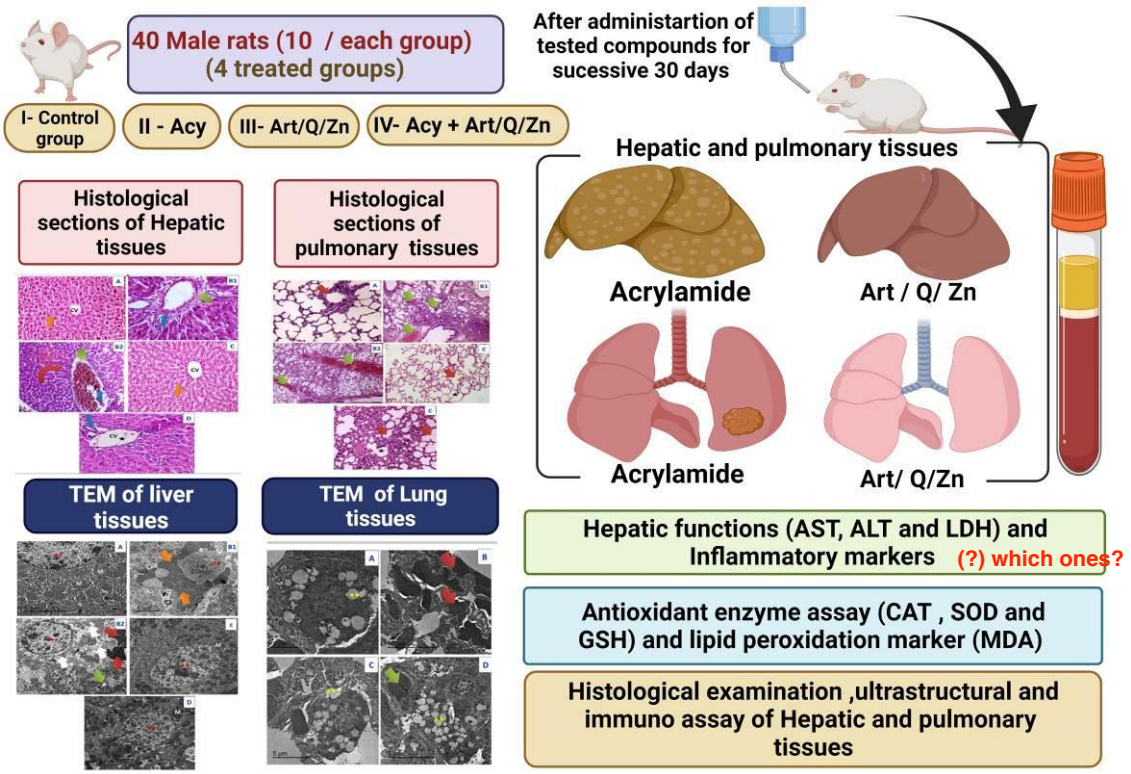

HE and TEM images do not have enough quality! if i zoom in there is nothing but pixels!

also, impossible to analyse these images here! it would be good to have them in full quality in the supplements - if not there yet - !

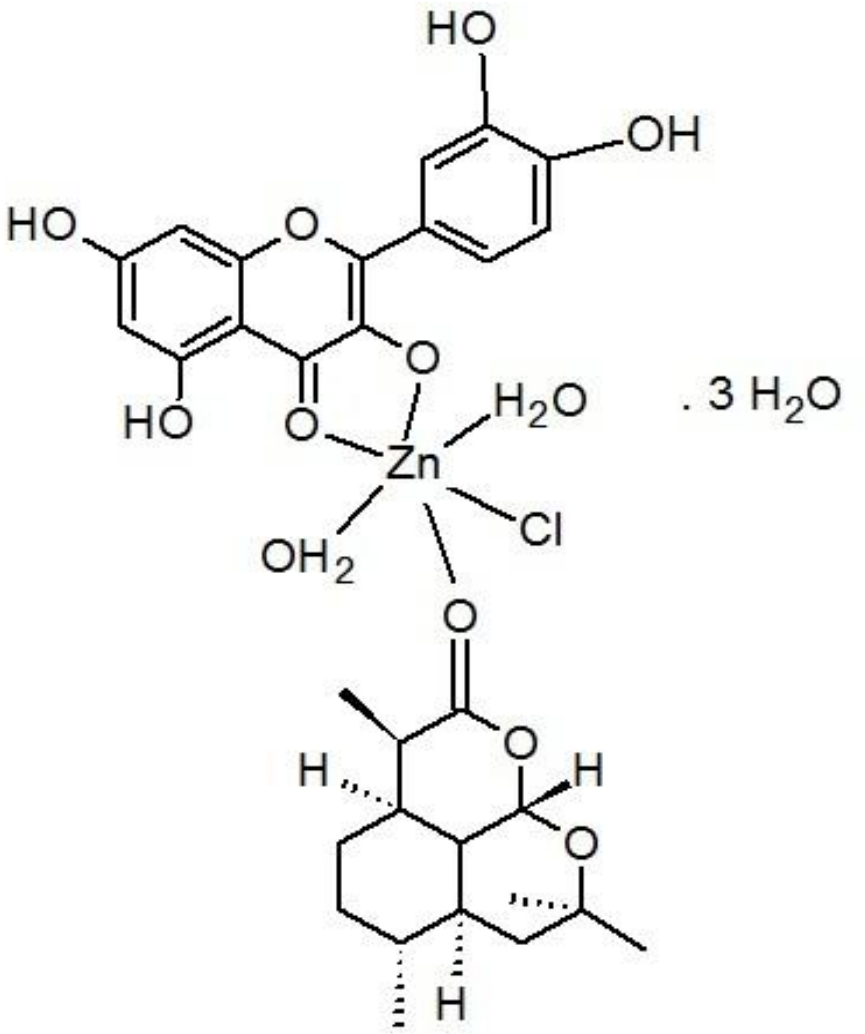
HO
OH
HO
O
O
HO
O
Zn
H_2O
. 3 H_2O
Cl
OH_2
O
O
H
H
O
H

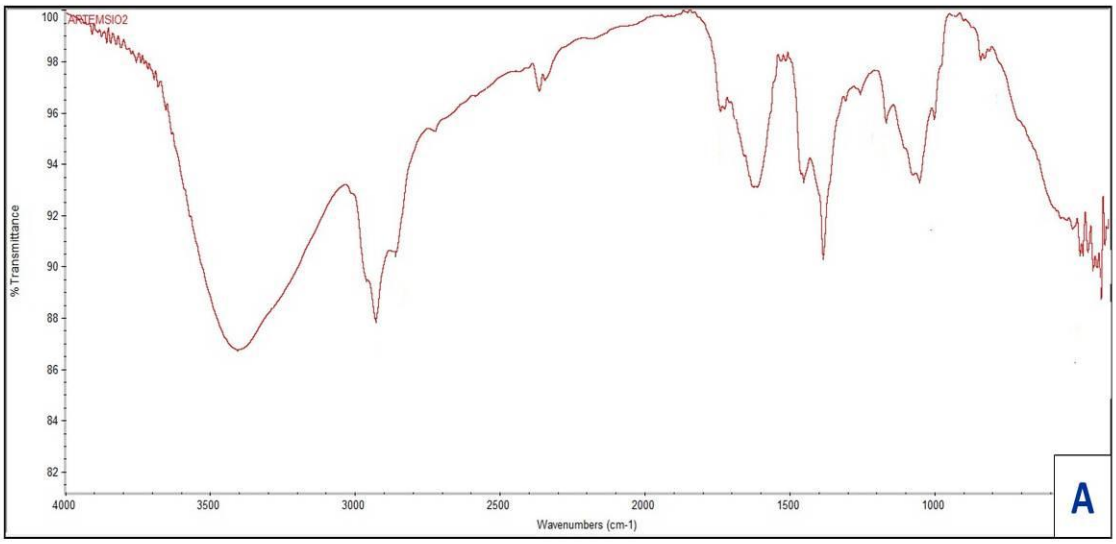
ARTEMSIO2
% Transmittance
Wavenumbers (cm-1)
A

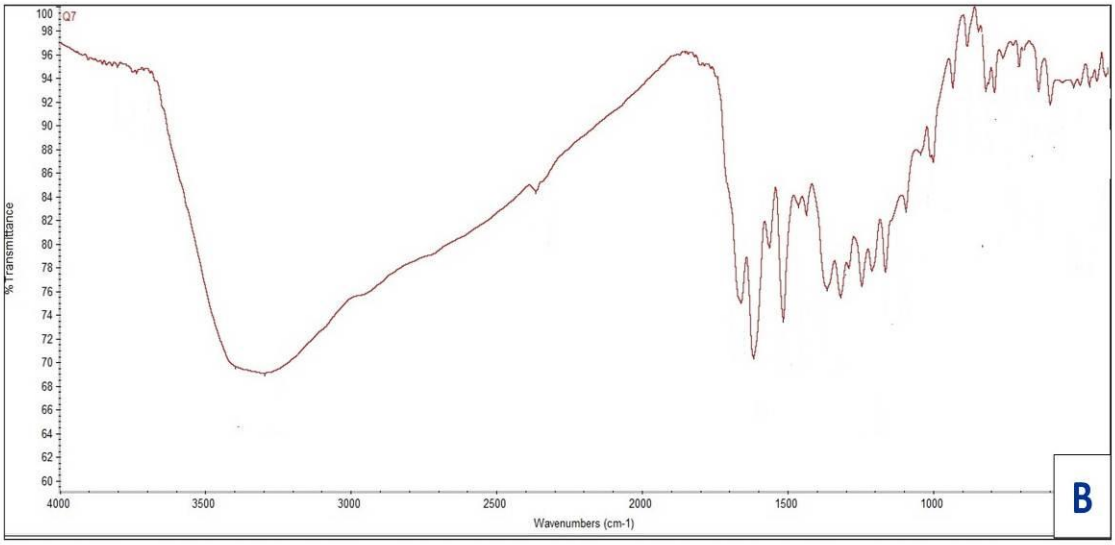
Q7
% Transmittance
Wavenumbers (cm-1)
B

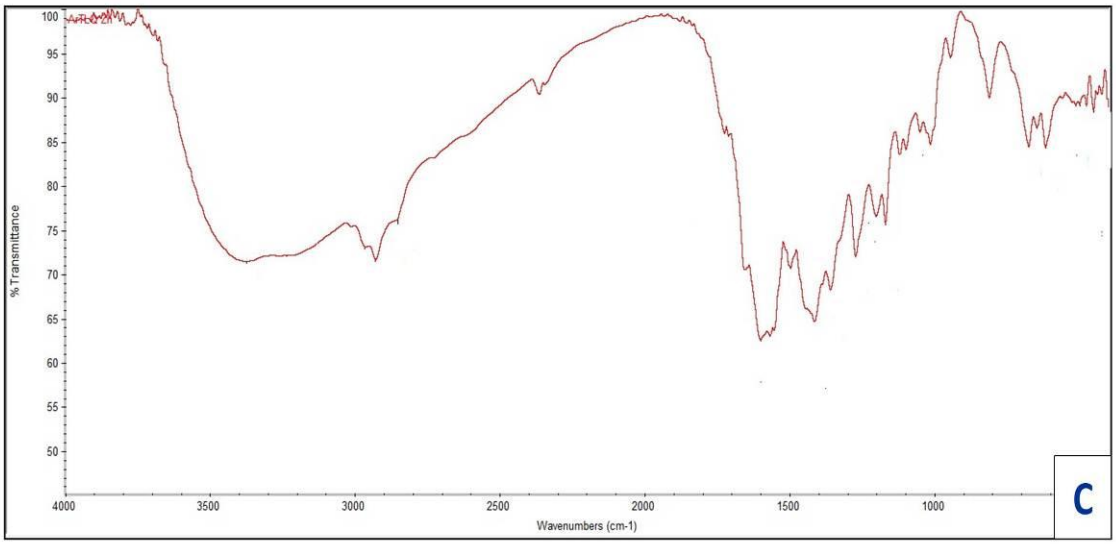
% Transmittance
Wavenumbers (cm-1)
C

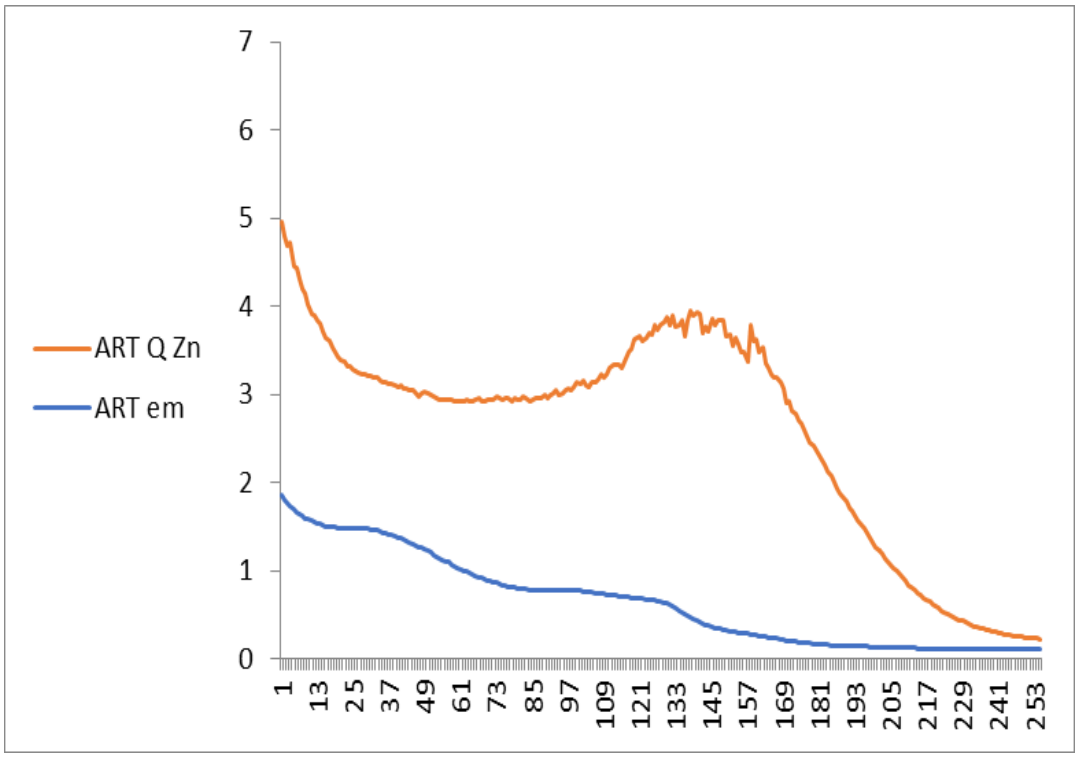

Axis need labels!!

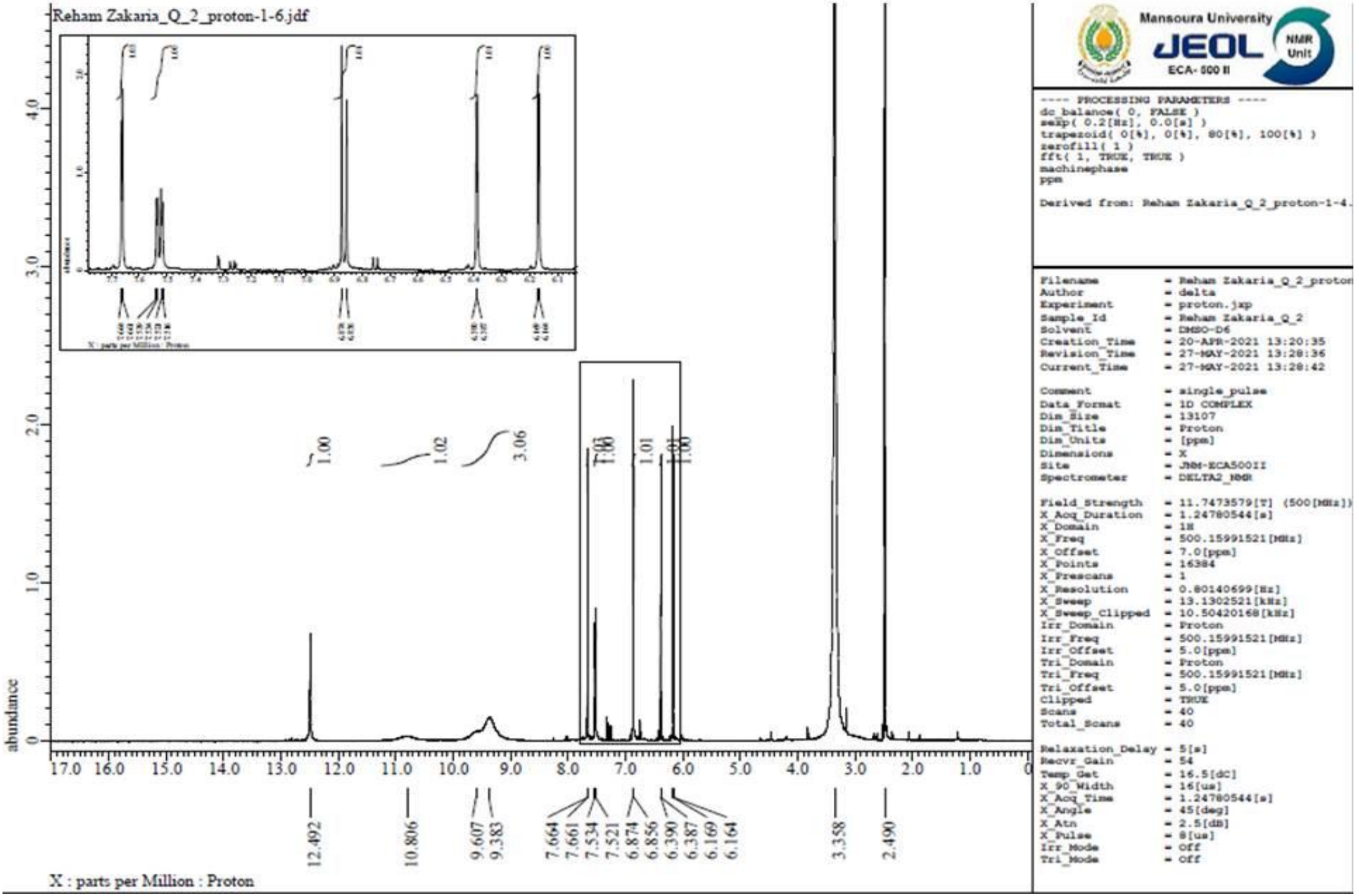
Reham Zakaria_Q_2_proton-1-6.jdf
Mansoura University
JEOL
ECA-500 II
NMR Unit
---- PROCESSING PARAMETERS ----
dc_balance(0, FALSE)
expo(0.2[Hz], 0.0[s])
trapezoid(0[%], 0[%], 80[%], 100[%])
zerofill(1)
fft(1, TRUE, TRUE)
machinephase
ppm
Derived from: Reham Zakaria_Q_2_proton-1-4.
Filename = Reham Zakaria_Q_2_proton
Author = delta
Experiment = proton.jxp
Sample_Id = Reham Zakaria_Q_2
Solvent = DMSO-D6
Creation_Time = 20-APR-2021 13:20:35
Revision_Time = 27-MAY-2021 13:28:36
Current_Time = 27-MAY-2021 13:28:42
Comment = single_pulse
Data_Format = 1D COMPLEX
Dim_Size = 13107
Dim_Title = Proton
Dim_Units = [ppm]
Dimensions = X
Site = JNM-ECA500II
Spectrometer = DELTA2_NMR
Field_Strength = 11.7473579[T] (500[MHz])
X_Acq_Duration = 1.24780544[s]
X_Domain = 1H
X_Freq = 500.15991521[MHz]
X_Offset = 7.0[ppm]
X_Points = 16384
X_Prescans = 1
X_Resolution = 0.80140699[Hz]
X_Sweep = 13.1302521[kHz]
X_Sweep_Clipped = 10.50420168[kHz]
Irr_Domain = Proton
Irr_Freq = 500.15991521[MHz]
Irr_Offset = 5.0[ppm]
Tri_Domain = Proton
Tri_Freq = 500.15991521[MHz]
Tri_Offset = 5.0[ppm]
Clipped = TRUE
Scans = 40
Total_Scans = 40
Relaxation_Delay = 5[s]
Recvr_Gain = 54
Temp_Get = 16.5[dC]
X_90_Width = 16[us]
X_Acq_Time = 1.24780544[s]
X_Angle = 45[deg]
X_Atn = 2.5[dB]
X_Pulse = 8[us]
Irr_Mode = Off
Tri_Mode = Off
abundance
1.00
1.02
3.06
1.01
12.492
10.806
9.607
9.383
7.664
7.661
7.534
7.521
6.874
6.856
6.390
6.387
6.169
6.164
3.358
2.490
X : parts per Million : Proton

(Coupled TwoTheta/Theta)

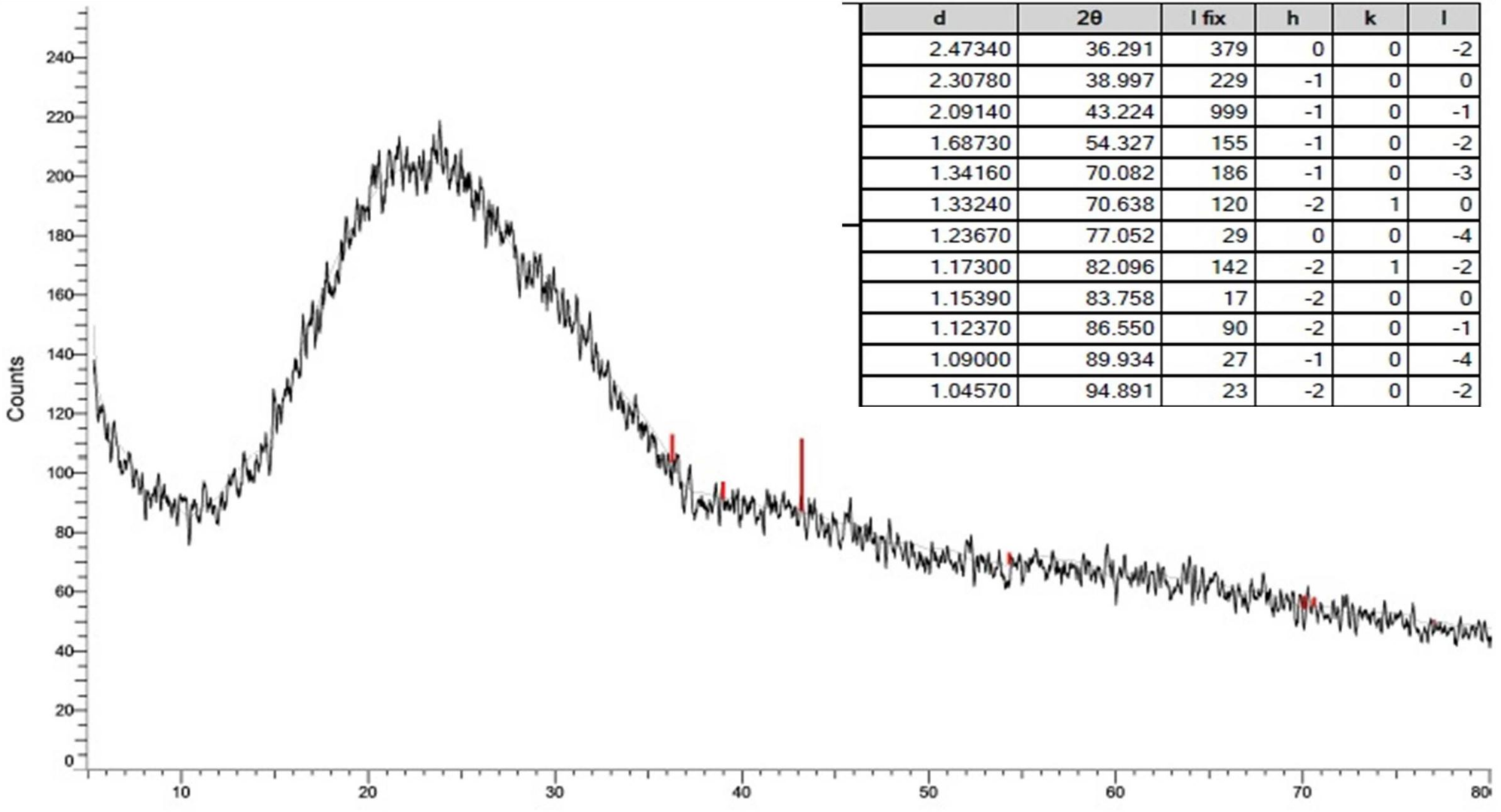

d	2θ	I fix	h	k	l
2.47340	36.291	379	0	0	-2
2.30780	38.997	229	-1	0	0
2.09140	43.224	999	-1	0	-1
1.68730	54.327	155	-1	0	-2
1.34160	70.082	186	-1	0	-3
1.33240	70.638	120	-2	1	0
1.23670	77.052	29	0	0	-4
1.17300	82.096	142	-2	1	-2
1.15390	83.758	17	-2	0	0
1.12370	86.550	90	-2	0	-1
1.09000	89.934	27	-1	0	-4
1.04570	94.891	23	-2	0	-2

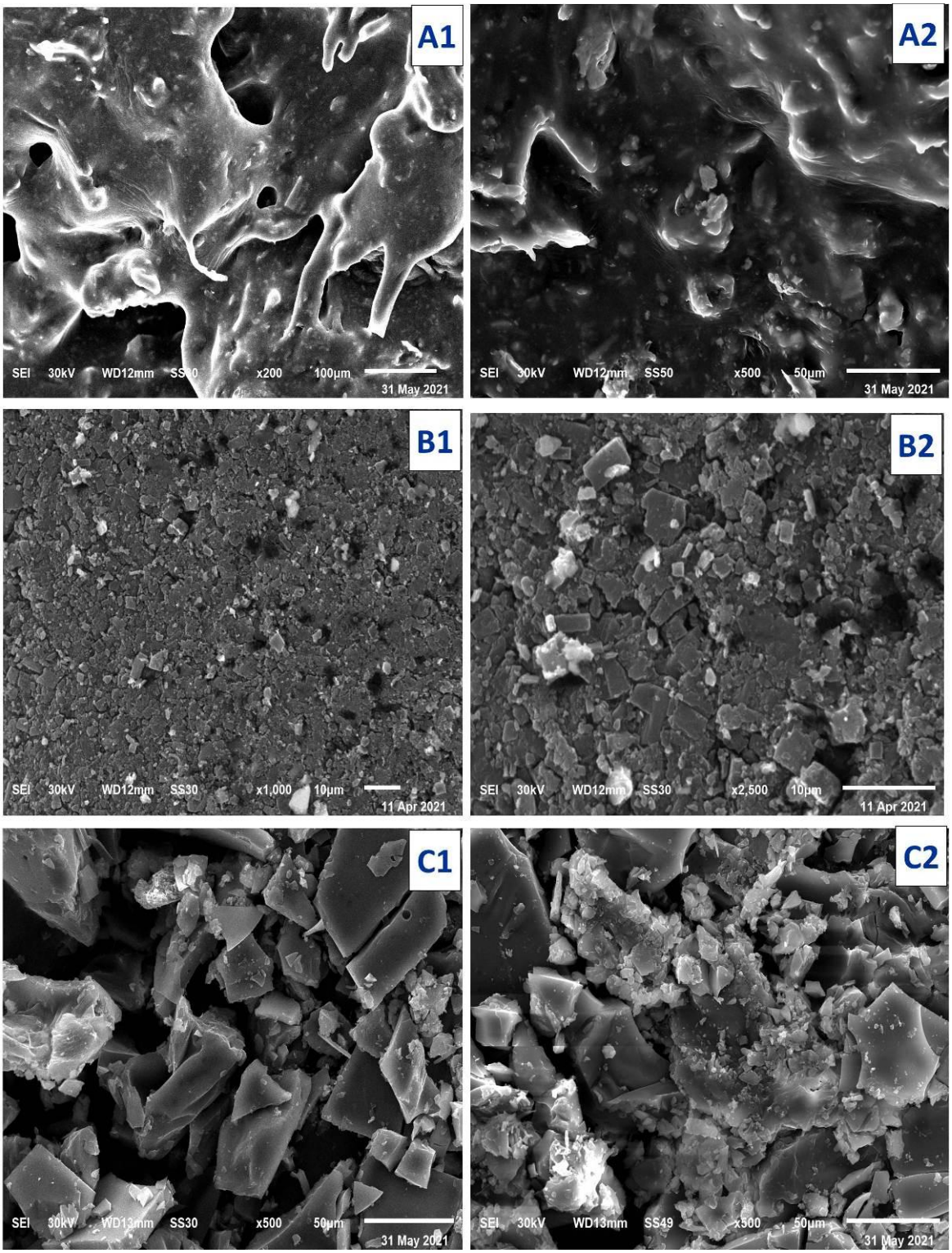
A1
SEI 30kV WD12mm SS30 x200 100µm
31 May 2021
A2
SEI 30kV WD12mm SS50 x500 50µm
31 May 2021
B1
SEI 30kV WD12mm SS30 x1,000 10µm
11 Apr 2021
B2
SEI 30kV WD12mm SS30 x2,500 10µm
11 Apr 2021
C1
SEI 30kV WD13mm SS30 x500 50µm
31 May 2021
C2
SEI 30kV WD13mm SS49 x500 50µm
31 May 2021

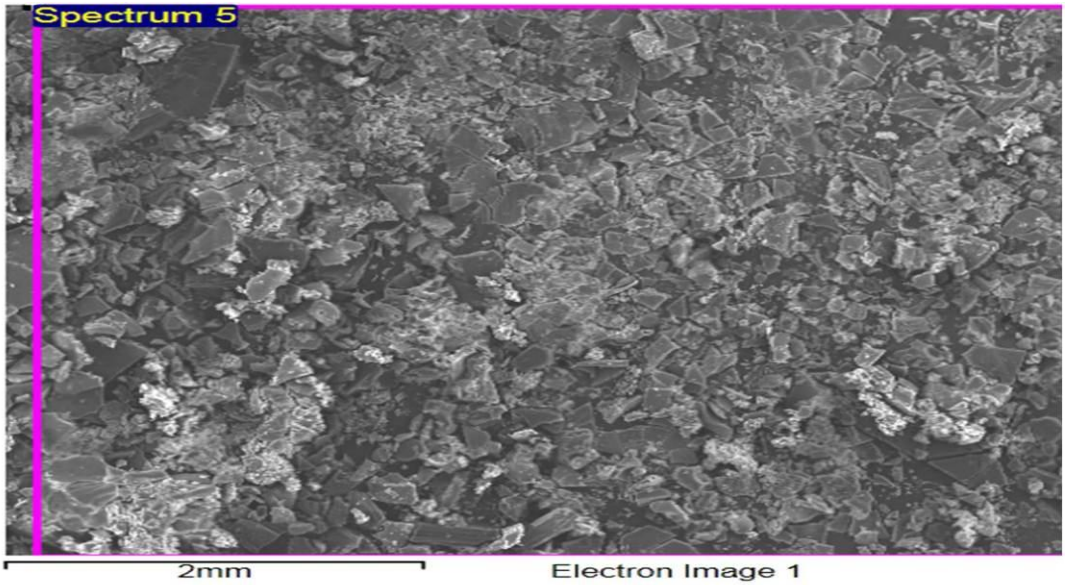

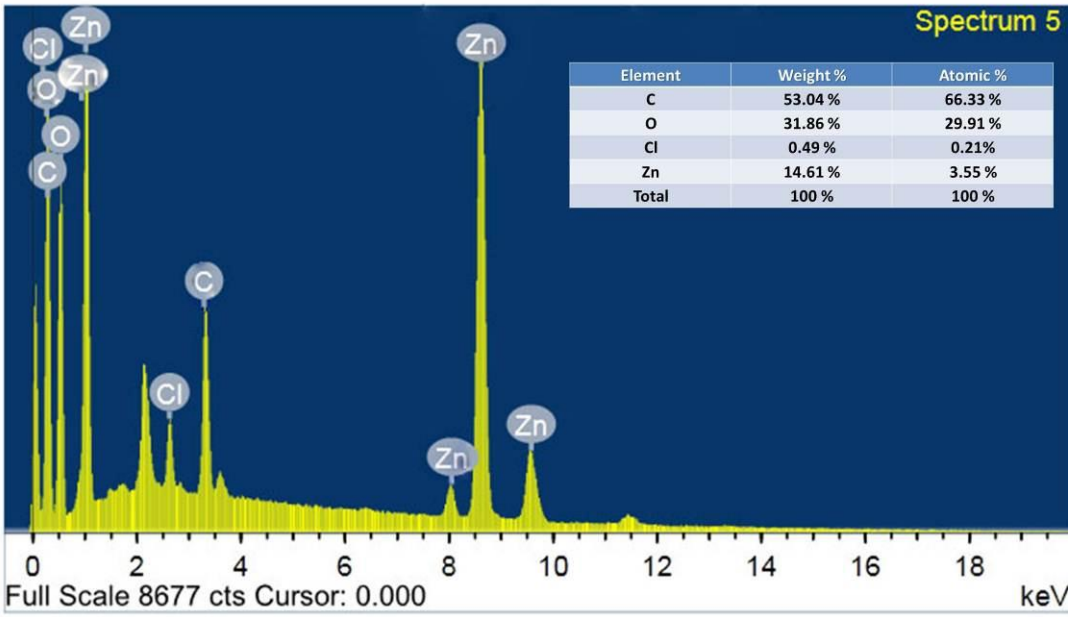

Element	Weight %	Atomic %
C	53.04 %	66.33 %
O	31.86 %	29.91 %
Cl	0.49 %	0.21%
Zn	14.61 %	3.55 %
Total	100 %	100 %

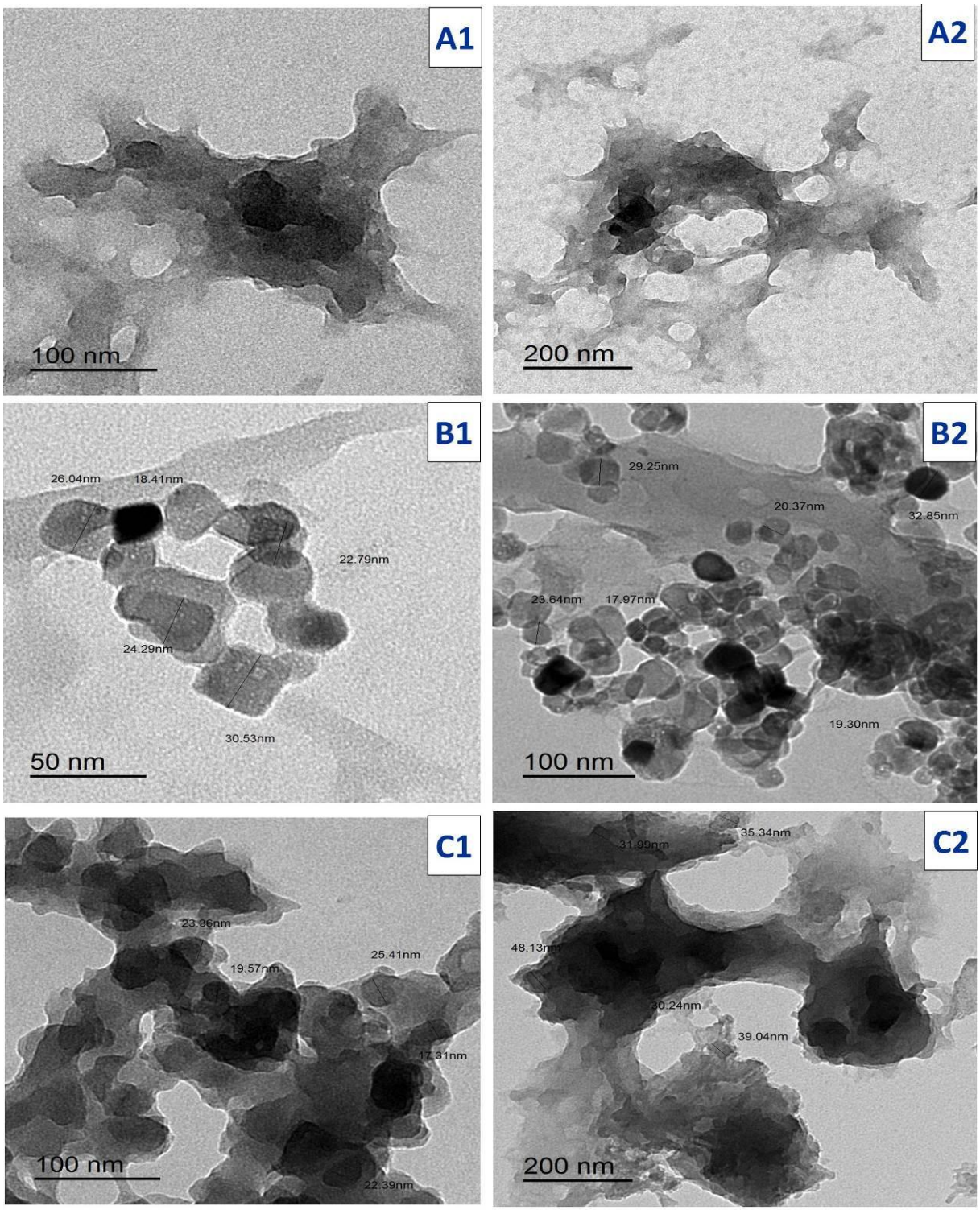
A1
100 nm
A2
200 nm
B1
26.04nm
18.41nm
22.79nm
24.29nm
30.53nm
50 nm
B2
29.25nm
20.37nm
32.85nm
23.64nm
17.97nm
19.30nm
100 nm
C1
23.36nm
19.57nm
25.41nm
17.31nm
100 nm
22.39nm
C2
31.99nm
35.34nm
48.13nm
30.24nm
39.04nm
200 nm

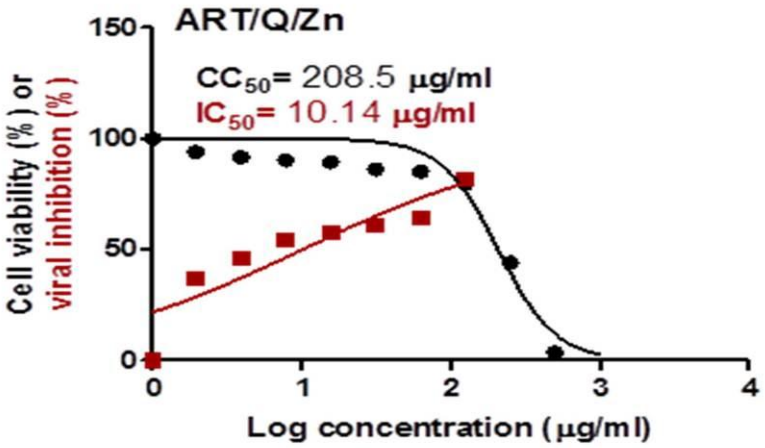
ART/Q/Zn
CC_{50}= 208.5 µg/ml
IC_{50}= 10.14 µg/ml
Cell viability (%) or
viral inhibition (%)
150
100
50
0
0
1
2
3
4
Log concentration (µg/ml)

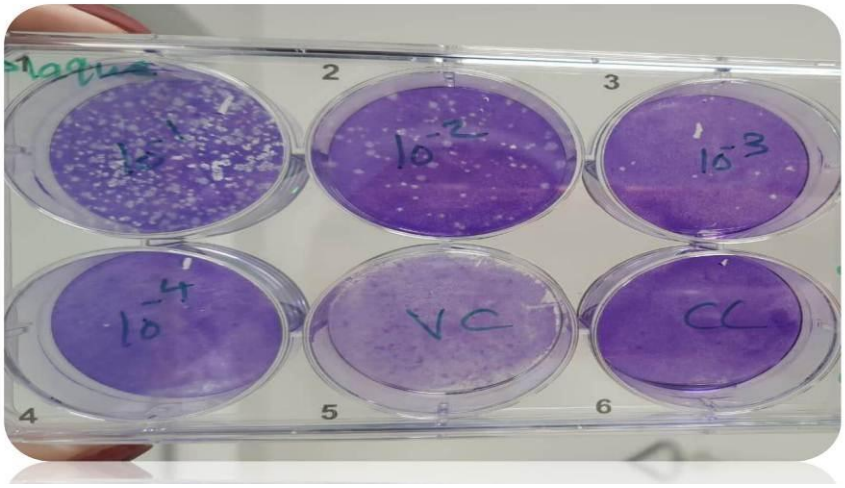
2
3
10^{-2}
10^{-3}
10^{-4}
VC
CC
4
5
6

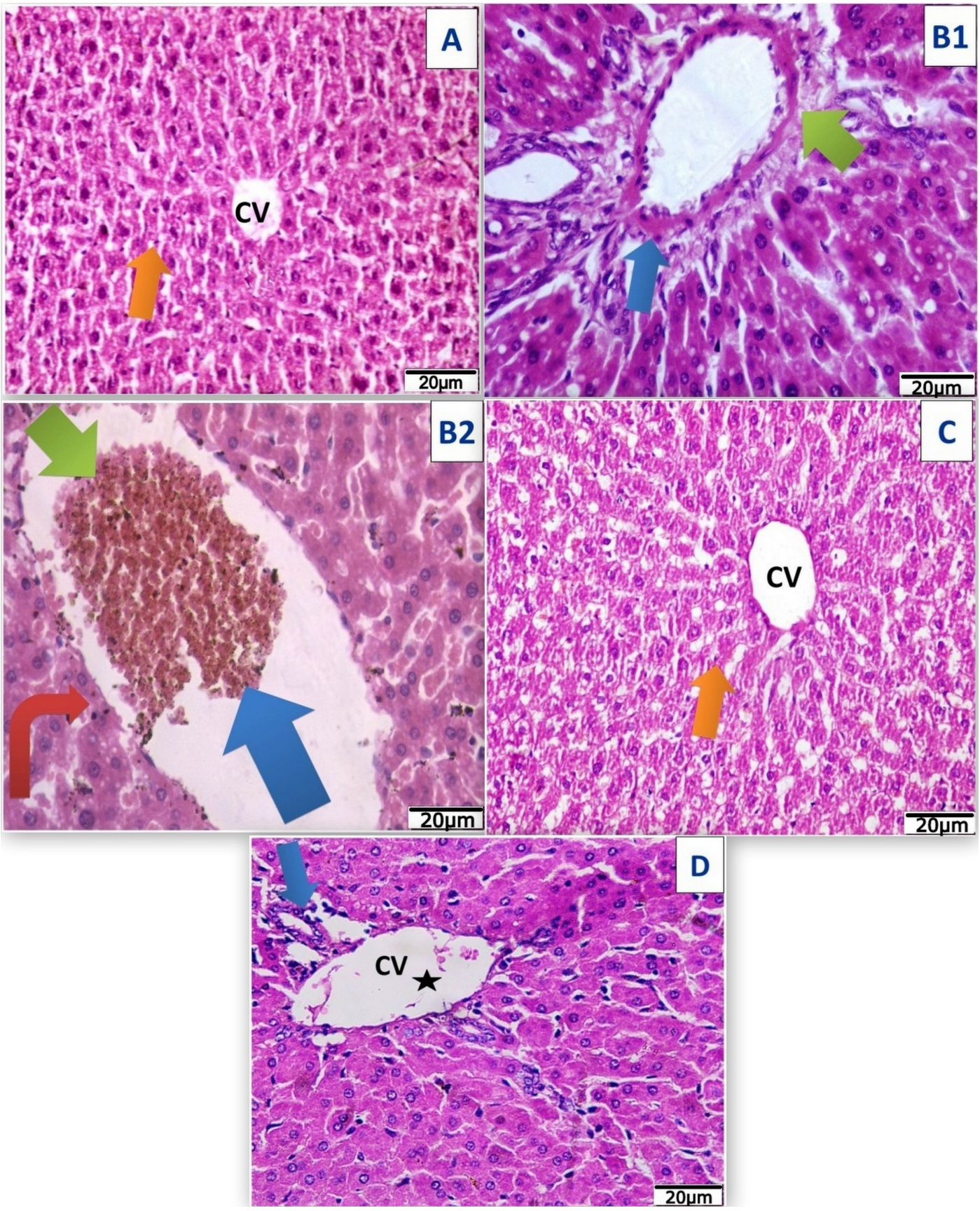
A
CV
20µm
B1
20µm
B2
20µm
C
CV
20µm
D
CV
20µm

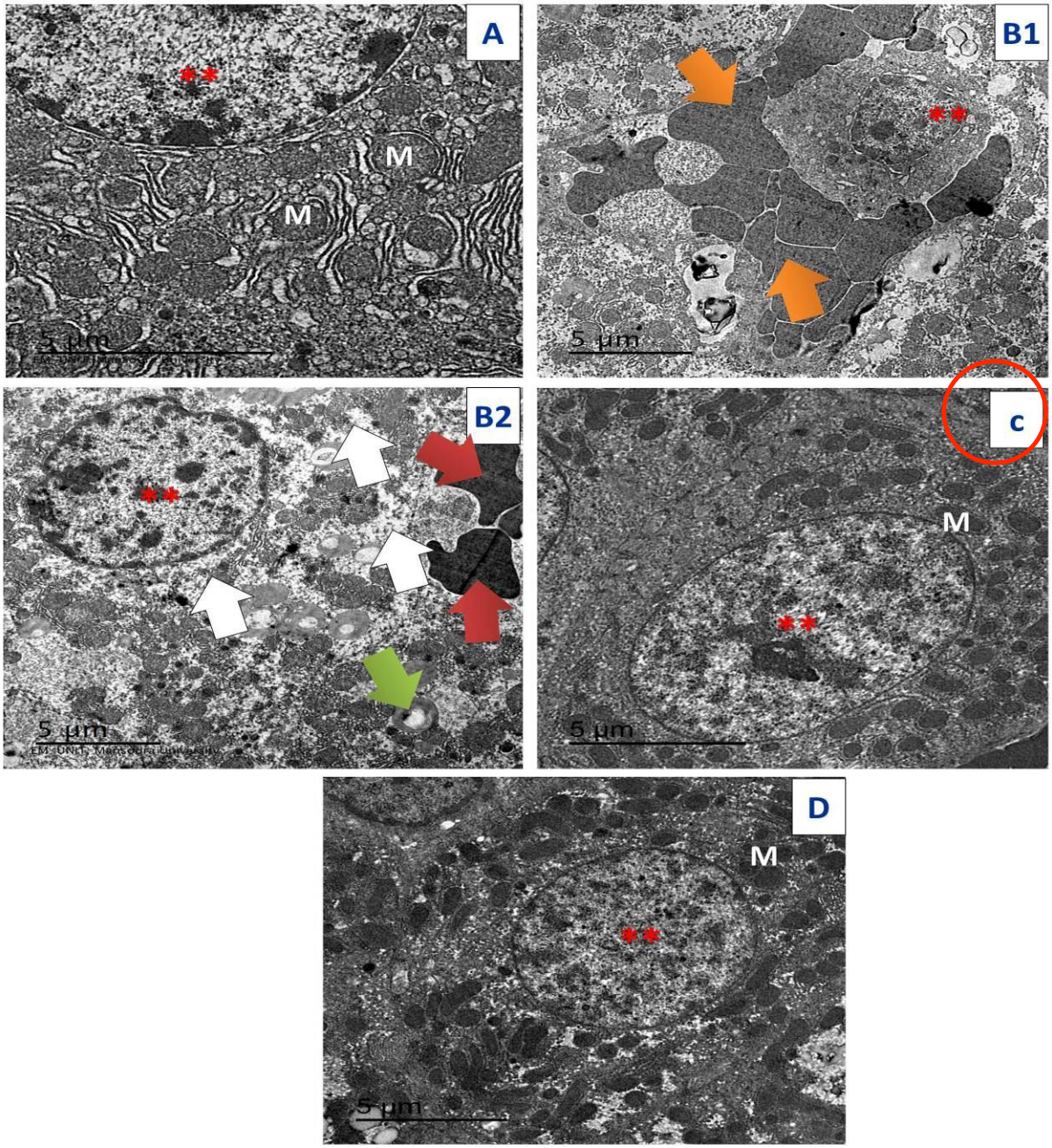

Capital C!

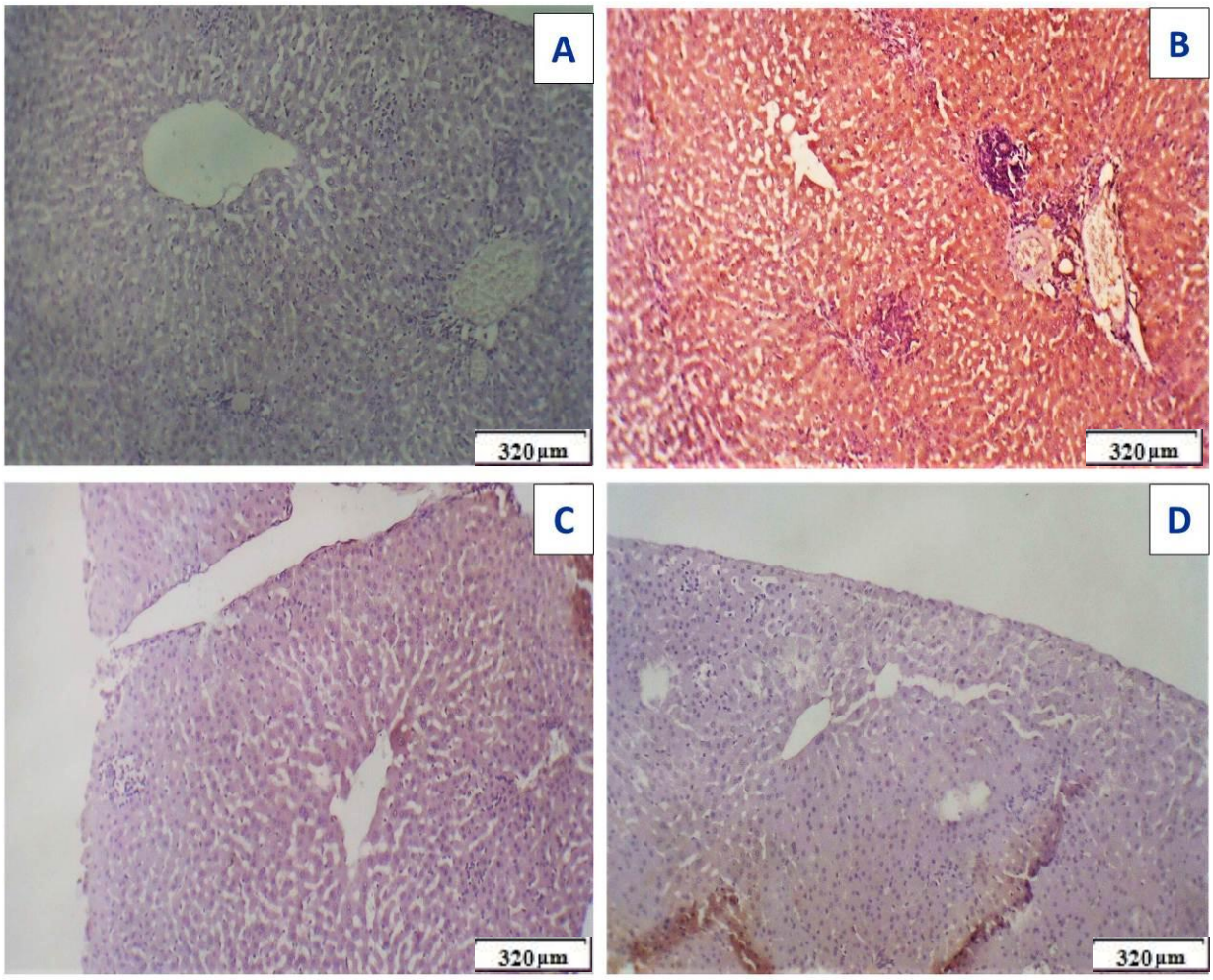
A
320 µm
B
320 µm
C
320 µm
D
320 µm

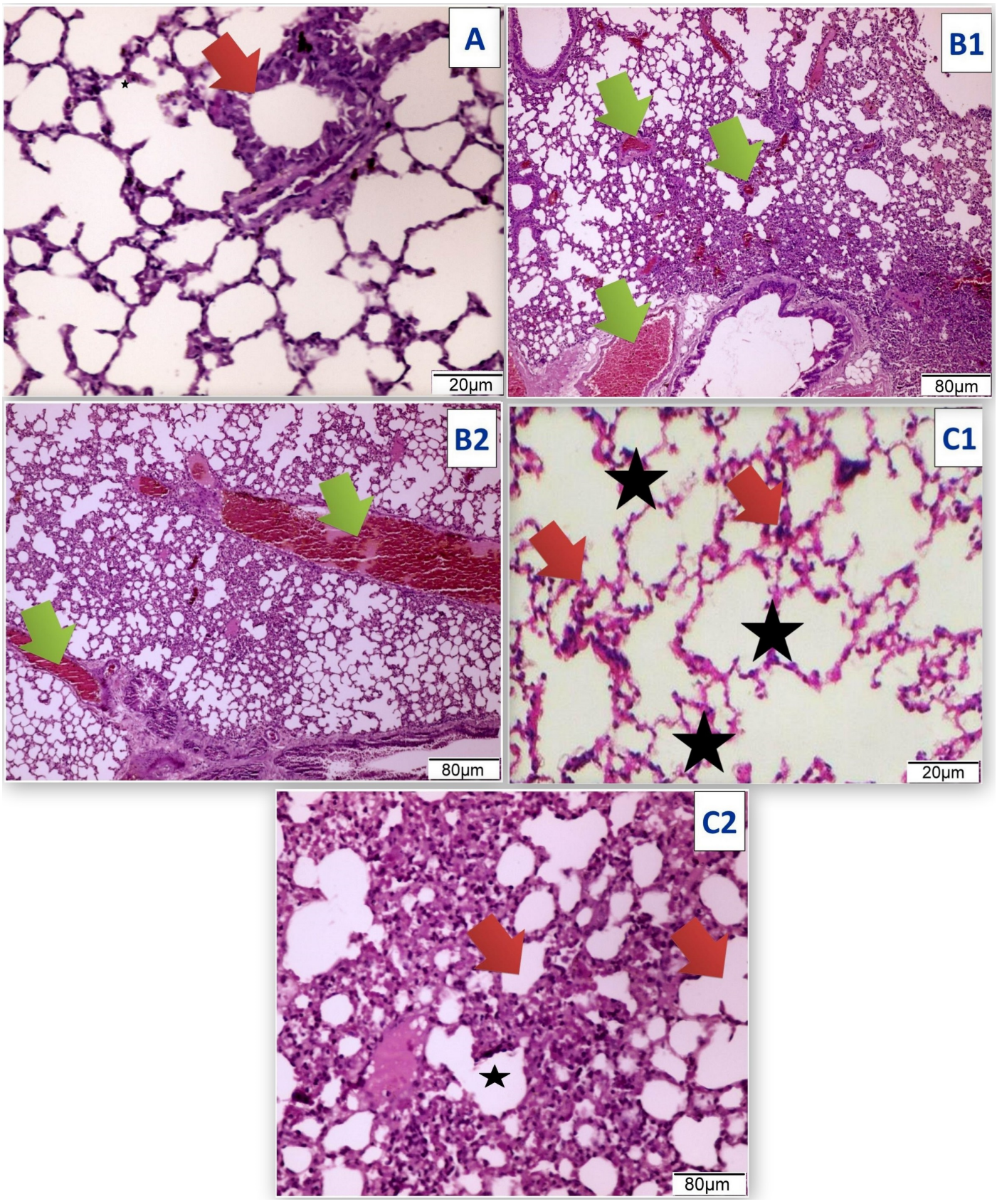
A
20μm
B1
80μm
B2
80μm
C1
20μm
C2
80μm

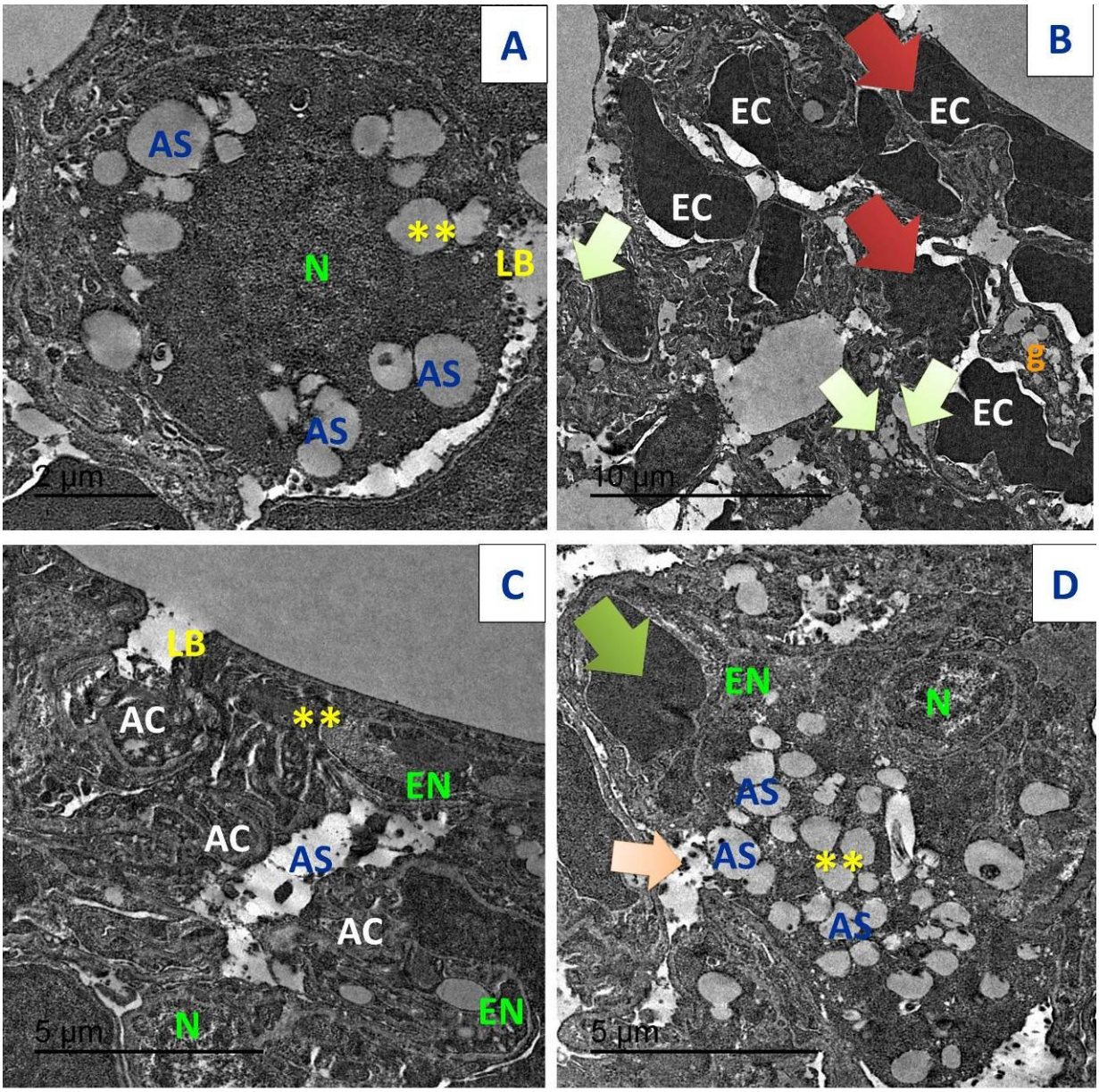
A
AS
**
N
LB
AS
AS
2 µm
B
EC
EC
EC
g
EC
10 µm
C
LB
AC
**
EN
AC
AS
AC
EN
N
5 µm
D
EN
N
AS
AS
**
AS
5 µm

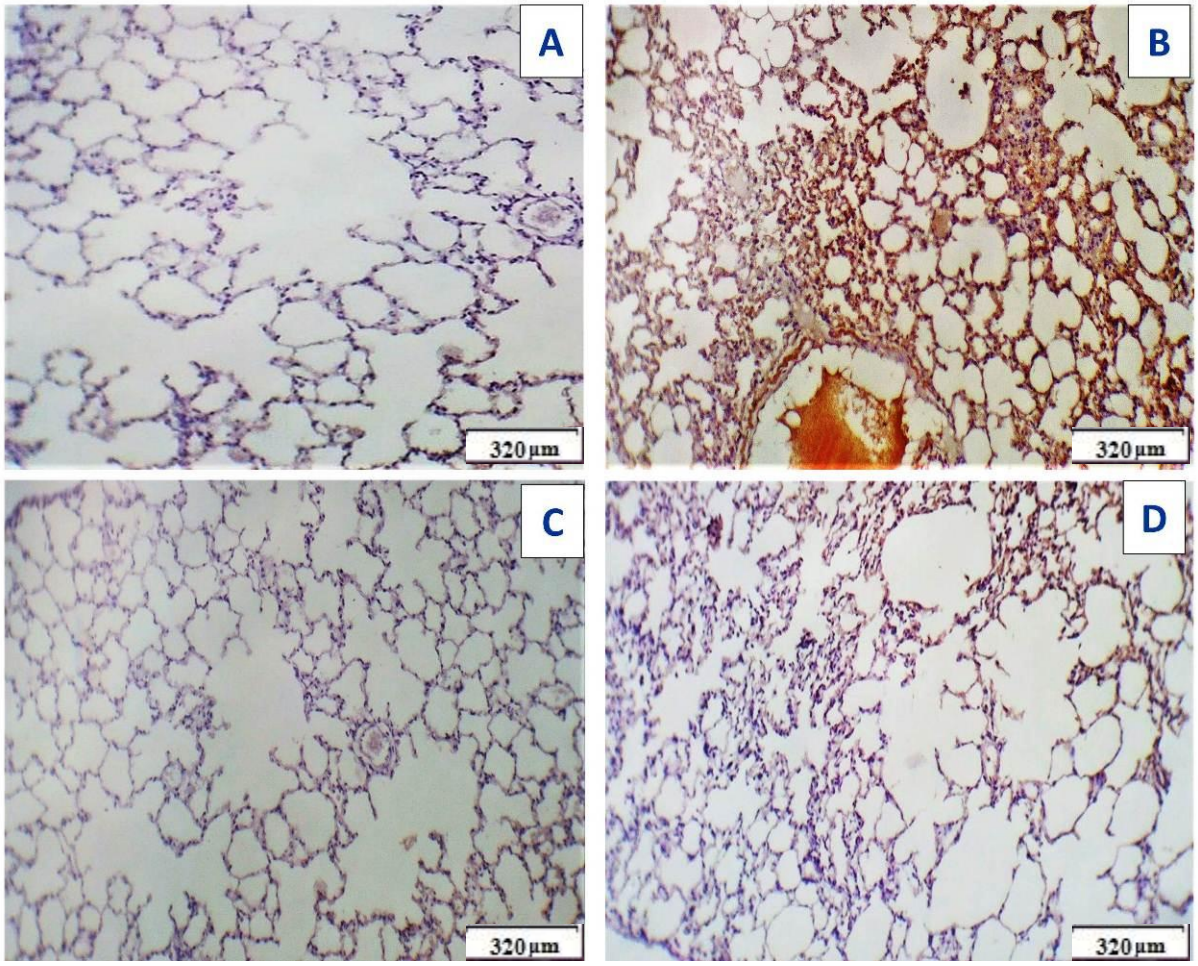
A
320 µm
B
320 µm
C
320 µm
D
320 µm

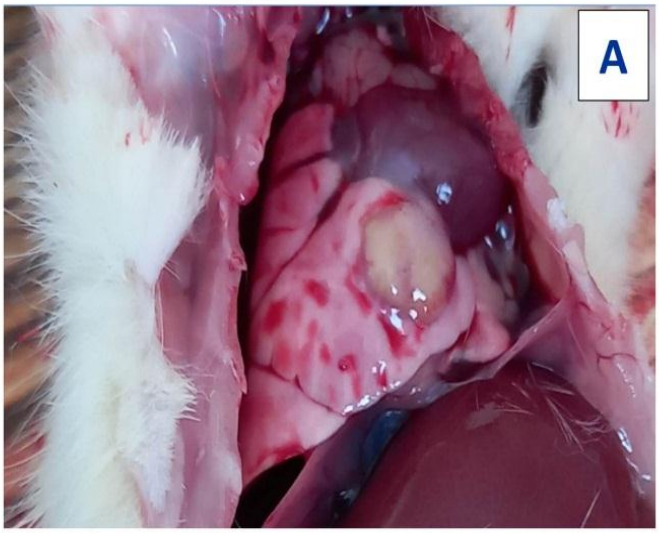
A


B


C1


C2


C3


D1


D2

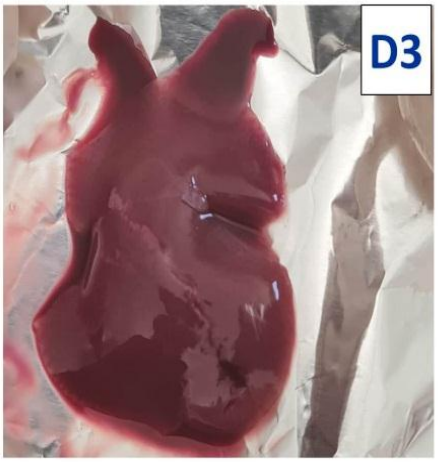
D3

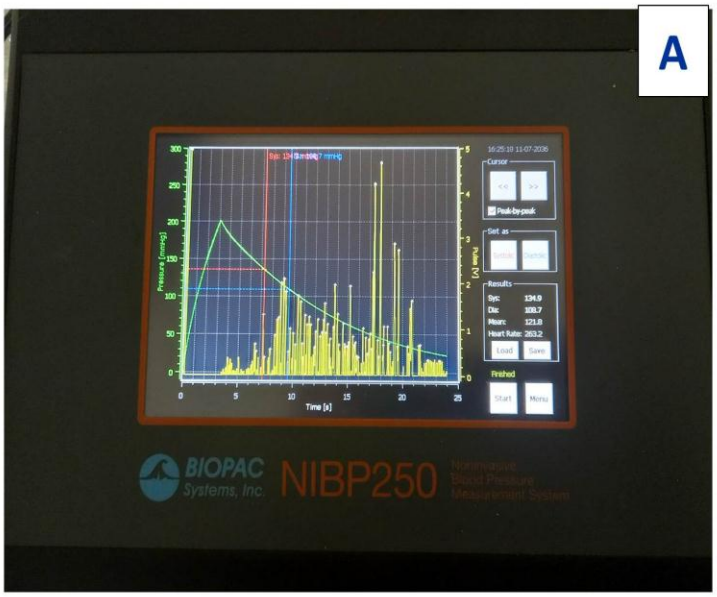
A
BIOPAC Systems, Inc.
NIBP250

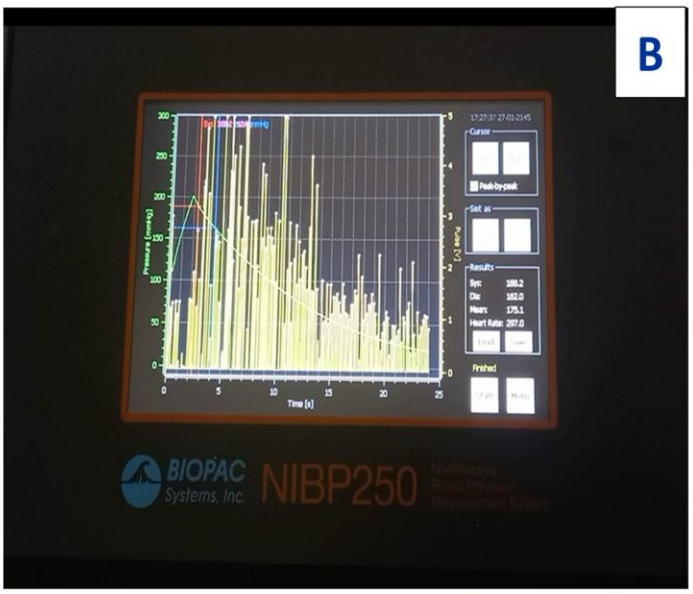
B
BIOPAC Systems, Inc.
NIBP250

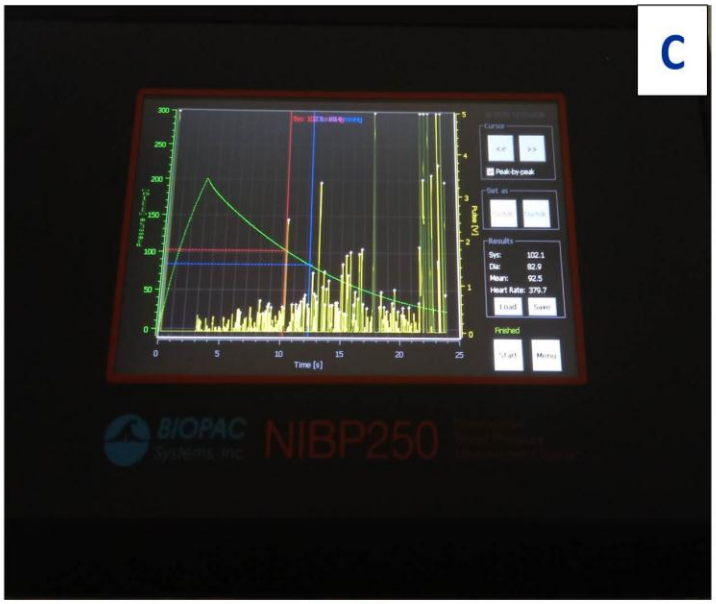
C
BIOPAC Systems, Inc.
NIBP250

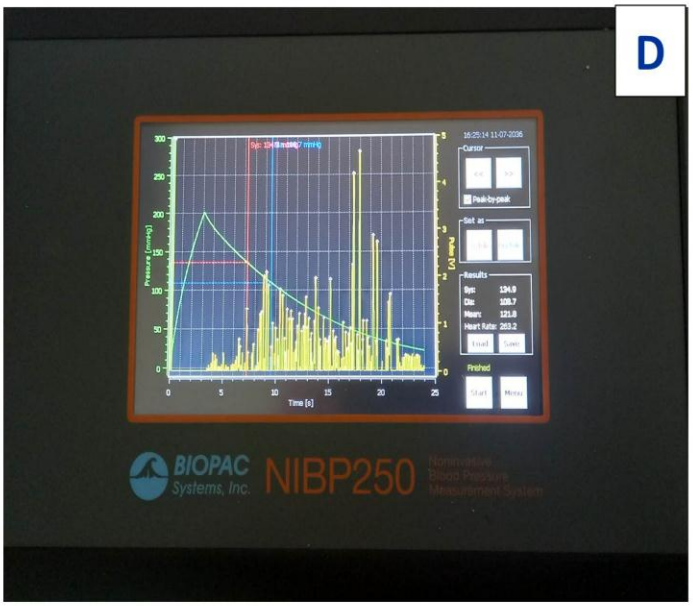
D
BIOPAC Systems, Inc.
NIBP250


E

A

3D Binding Interaction (Art/Q/Zn)

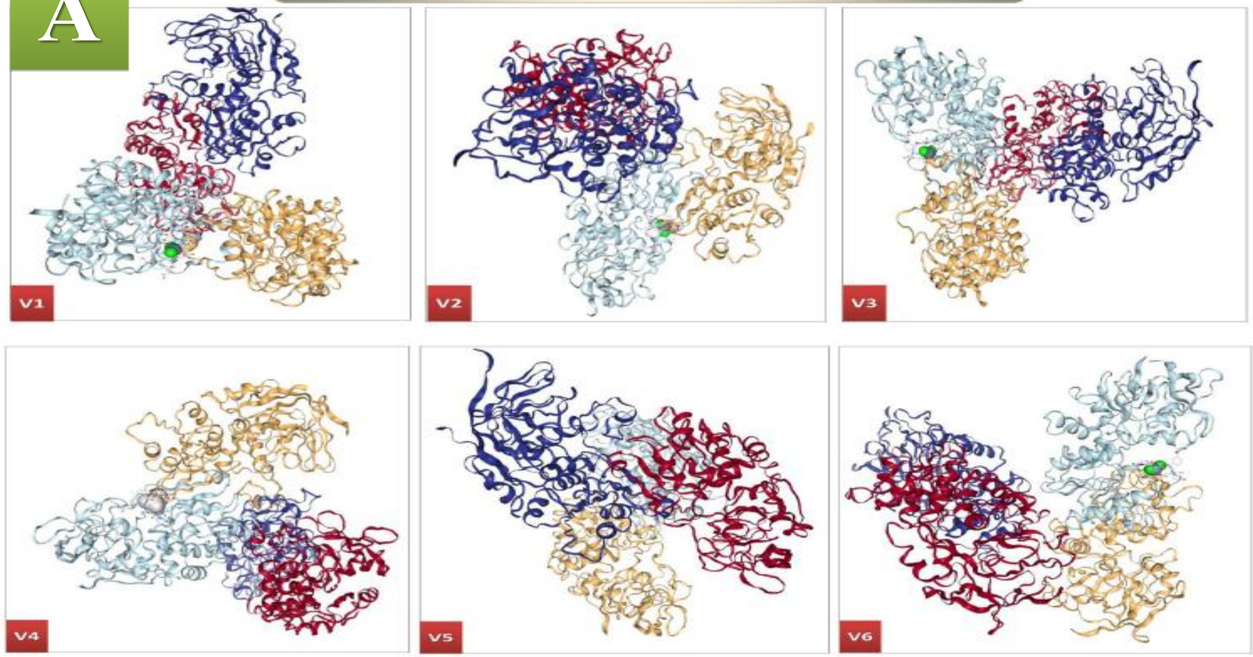

B

Simulation of novel complex of (Art/Q/Zn) with ACE2 receptor

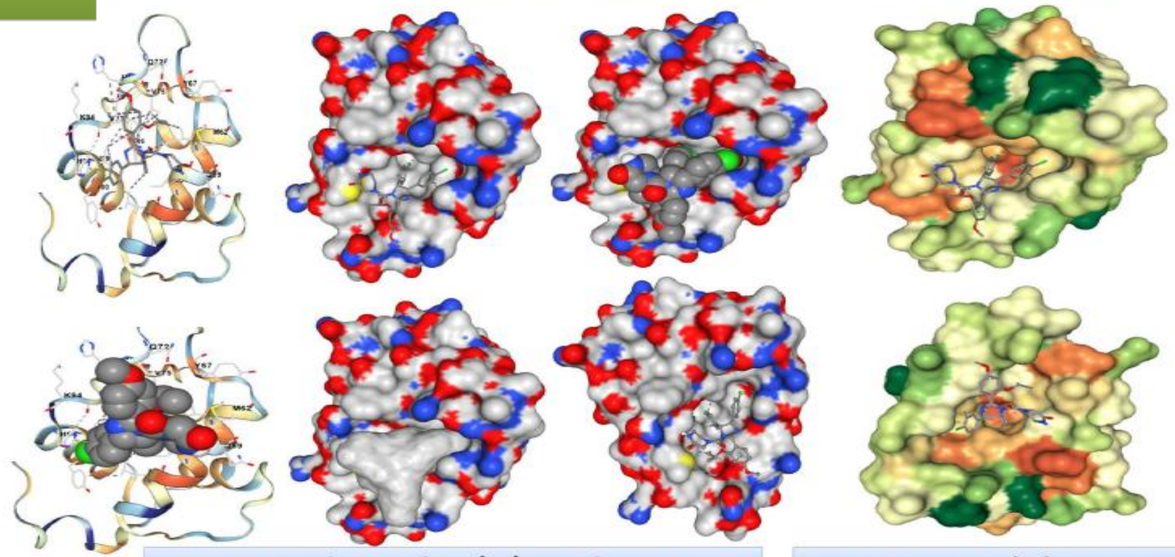

3D Simulation of Art/Q/Zn with ACE2

Lipophilicity of Art/Q/Zn with ACE2

C

Simulation of novel complex of (Art/Q/Zn) with MPro receptor

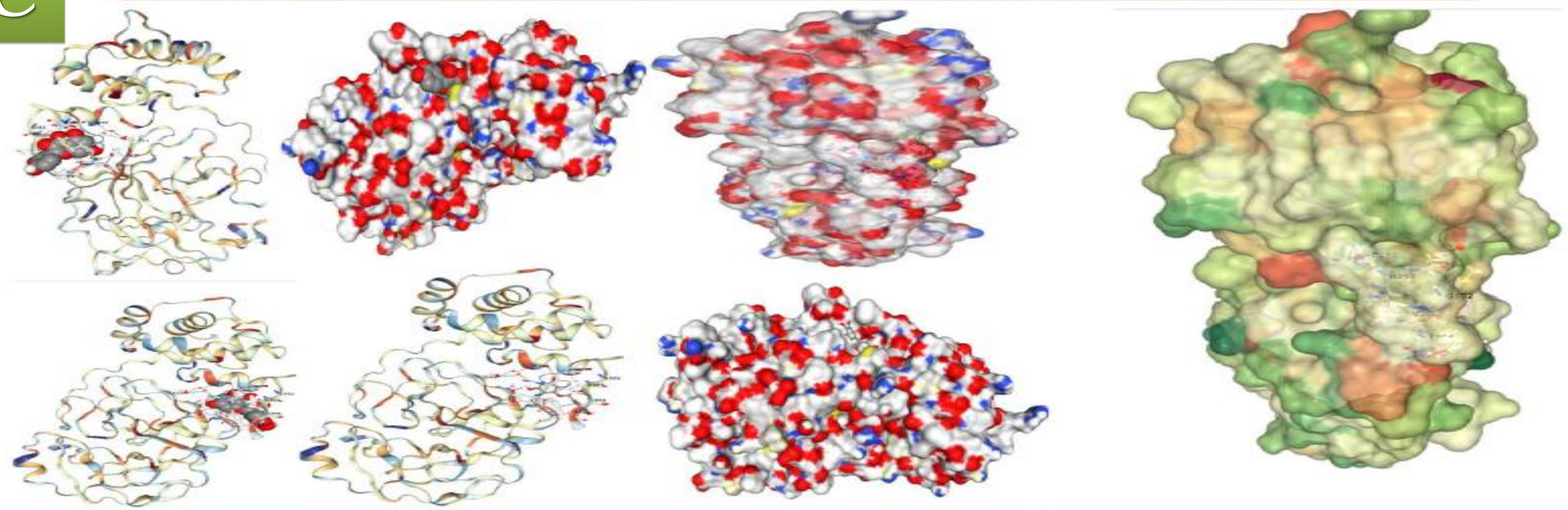

3D Simulation of Art/Q/Zn with MPro

Lipophilicity of Art/Q/Zn with MPro

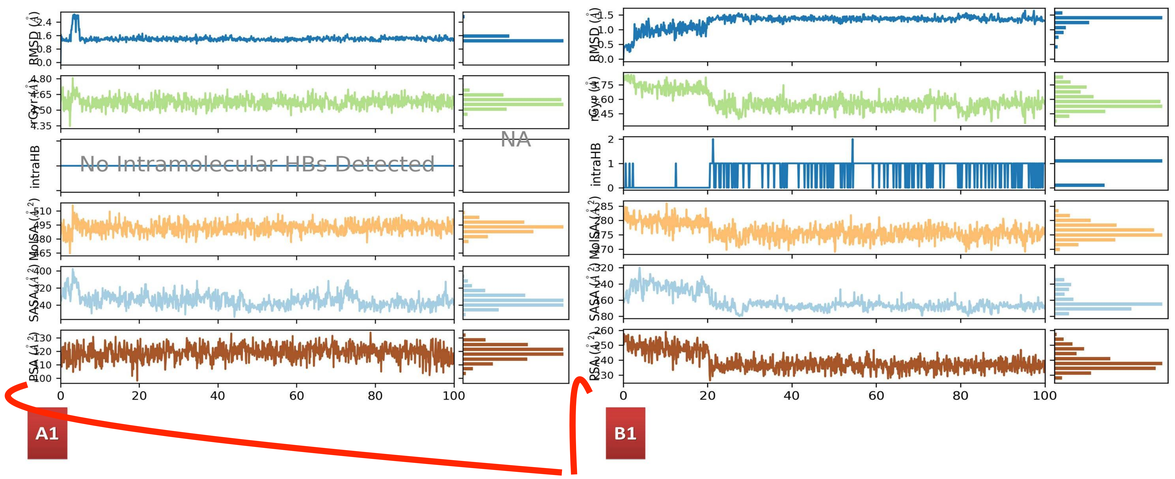

A1

B1

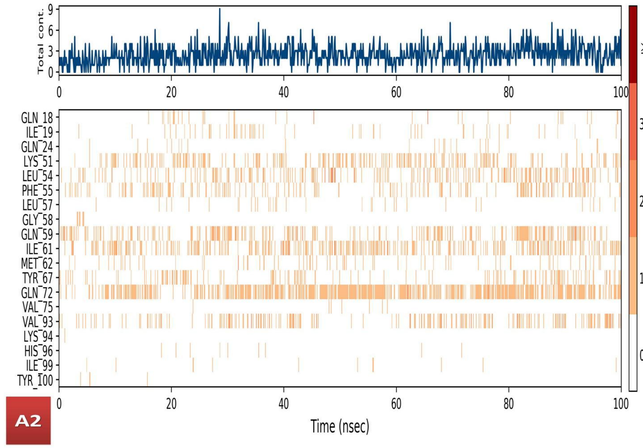

A2

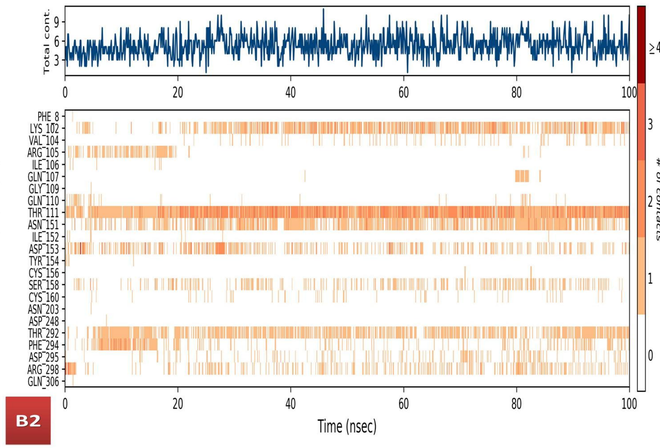

B2

text overlap!

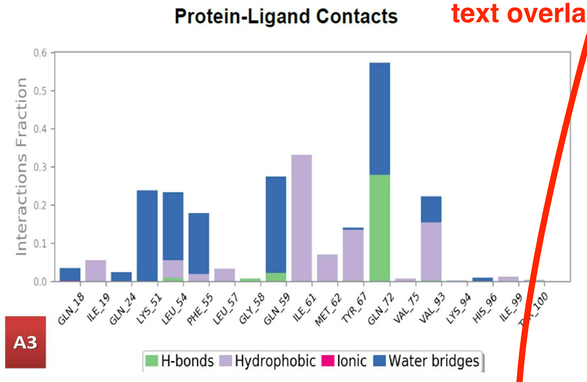

A3

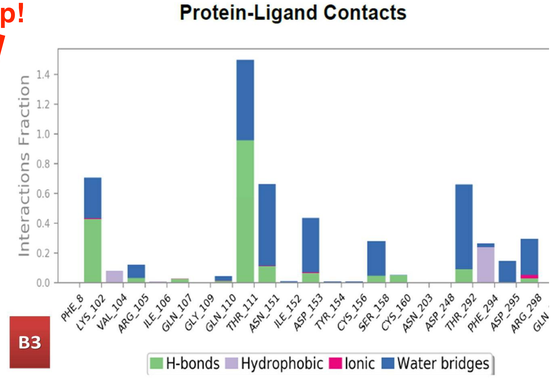

B3

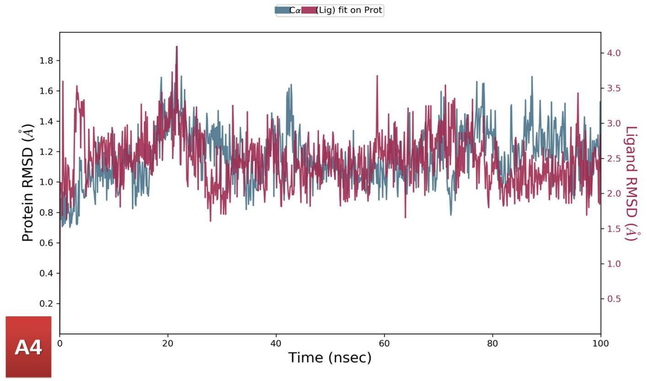

A4

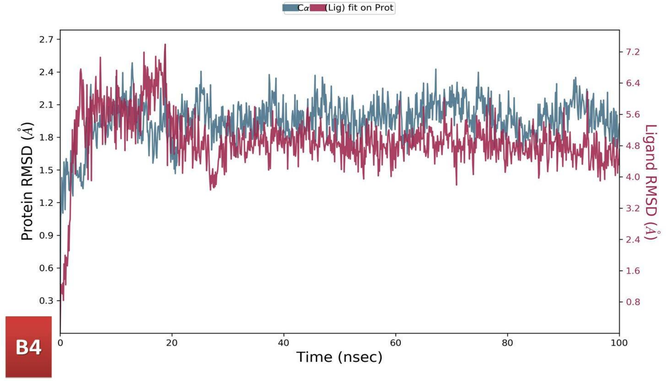

B4

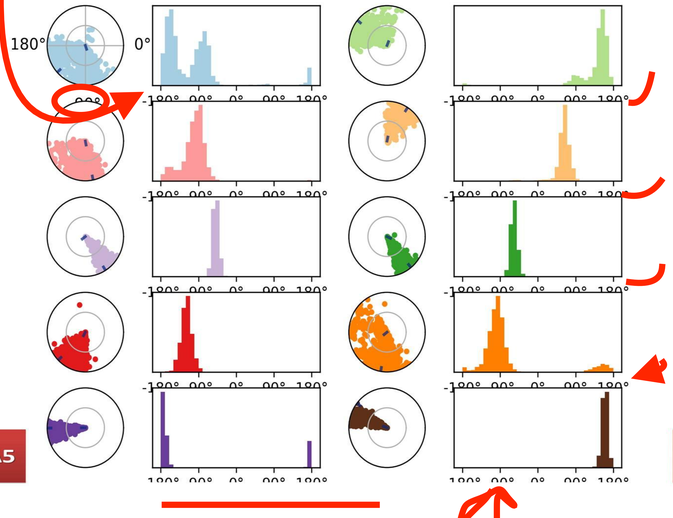

A5

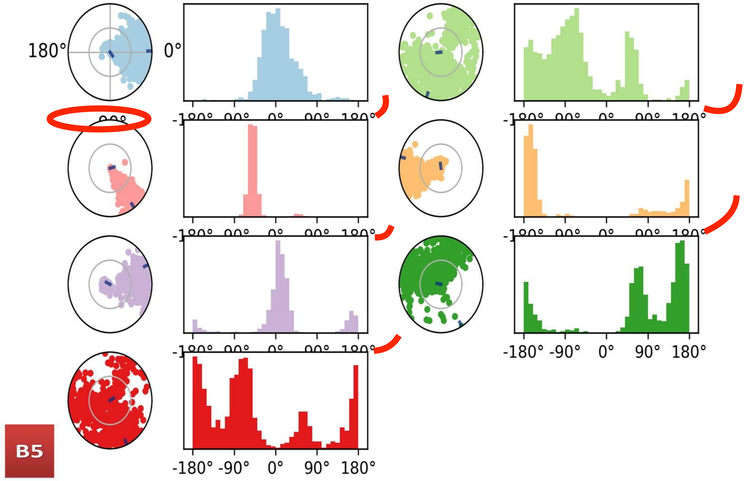

B5

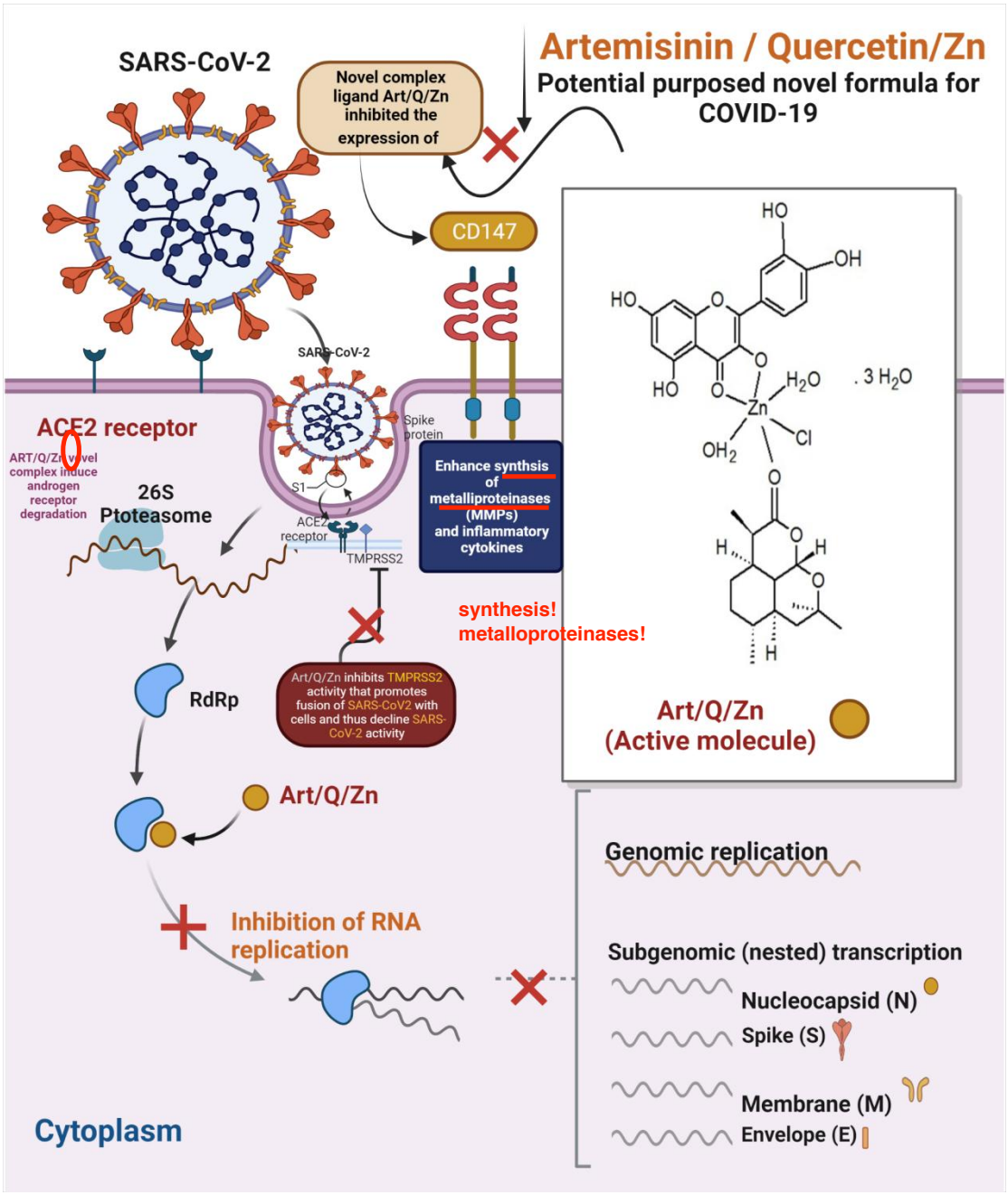
Artemisinin / Quercetin/Zn
Potential purposed novel formula for COVID-19
SARS-CoV-2
Novel complex ligand Art/Q/Zn inhibited the expression of
CD147
SARS-CoV-2
Spike protein
ACE2 receptor
ART/Q/Zn novel complex induce androgen receptor degradation
26S Ptoteasome
S1
ACE2 receptor
TMPRSS2
Enhance synthsis of metalliproteinases (MMPs) and inflammatory cytokines
synthesis!
metalloproteinases!
novel!
RdRp
Art/Q/Zn inhibits TMPRSS2 activity that promotes fusion of SARS-CoV2 with cells and thus decline SARS-CoV-2 activity
Art/Q/Zn
Art/Q/Zn (Active molecule)
Inhibition of RNA replication
Genomic replication
Subgenomic (nested) transcription
Nucleocapsid (N)
Spike (S)
Membrane (M)
Envelope (E)
Cytoplasm